Available online at www.sciencedirect.com
ScienceDirect
Marine Chemistry 109 (2008) 355–376
MARINE CHEMISTRY
www.elsevier.com/locate/marchem

Submarine groundwater discharge and nutrient addition to the coastal zone and coral reefs of leeward Hawai'i

Joseph H. Street [a,*], Karen L. Knee [a], Eric E. Grossman [b], Adina Paytan [a]

[a] Department of Geological & Environmental Sciences, Stanford University, Bldg. 320, Rm. 118 450 Serra Mall, Stanford, CA 94305, USA
[b] Coastal and Marine Geology Program, U.S. Geological Survey Pacific Science Center, 400 Natural Bridges Dr. Santa Cruz, CA 95060, USA

Received 15 March 2007; received in revised form 28 August 2007; accepted 31 August 2007
Available online 7 September 2007

Abstract

Multiple tracers of groundwater input (salinity, Si, ^{223}Ra, ^{224}Ra, and ^{226}Ra) were used together to determine the magnitude, character (meteoric versus seawater), and nutrient contribution associated with submarine groundwater discharge across the leeward shores of the Hawai'ian Islands Maui, Moloka'i, and Hawai'i. Tracer abundances were elevated in the unconfined coastal aquifer and the nearshore zone, decreasing to low levels offshore, indicative of groundwater discharge (near-fresh, brackish, or saline) at all locations. At several sites, we detected evidence of fresh and saline SGD occurring simultaneously. Conservative estimates of SGD fluxes ranged widely, from 0.02–0.65 $m^3\ m^{-2}\ d^{-1}$at the various sites. Groundwater nutrient fluxes of 0.04–40 mmol N $m^{-2}\ d^{-1}$ and 0.01–1.6 mmol P $m^{-2}\ d^{-1}$ represent a major source of new nutrients to coastal ecosystems along these coasts. Nutrient additions were typically greatest at locations with a substantial meteoric component in groundwater, but the recirculation of seawater through the aquifer may provide a means of transferring terrestrially-derived nutrients to the coastal zone at several sites.

Keywords: Submarine groundwater discharge; Coastal zone; Nutrients; Tracers; Radium isotopes; Hawai'i

1. Introduction

Submarine groundwater discharge (SGD) is an important source of new nutrients, trace elements, and contaminants to the coastal ocean in many parts of the world (e.g., Valiela et al., 1990a; Umezawa et al., 2002; Paytan et al., 2006). Rather than a unidirectional flow from land to sea, SGD is better described as an exchange of fluid between the coastal ocean and adjoining aquifers, in which discharge to the ocean consists of a spatially and temporally variable mixture of fresh meteoric groundwater and recirculated seawater (Moore 1999). Because groundwater nutrient concentrations are typically high relative to seawater, even small groundwater fluxes may make large contributions to coastal nutrient budgets (Li et al., 1999), particularly in oligotrophic areas with few other external nutrient sources (Shellenbarger et al., 2006).

Coral reefs, though highly productive ecosystems, typically occur in low-nutrient coastal waters and thus in some cases may be supported in part by nutrients delivered through SGD (Hatcher, 1997; Umezawa et al., 2002; Paytan et al., 2006). In areas where natural groundwater nutrient loads are augmented by anthropogenic sources such as sewage or fertilizer application, SGD may play a role in coastal eutrophication and reef degradation (D'Elia et al., 1981, Lapointe and O'Connell 1989, Valiela et al., 1990a,b; Lapointe 1997). Nearshore

* Corresponding author. Department of Geological & Environmental Sciences, Stanford University Stanford, CA 94305 USA. Tel.: +1 650 736 0655; fax: +1 650 725 2199.
E-mail address: jstreet@stanford.edu (J.H. Street).

0304-4203/$ - see front matter © 2007 Elsevier B.V. All rights reserved.
doi:10.1016/j.marchem.2007.08.009

fringing reefs are abundant in the Hawai'ian Islands and represent an important biological and economic resource (Cesar and Van Beukering 2004). As coastal development increases there is an urgent need to establish baseline environmental conditions and estimate natural and anthropogenic fluxes of nutrients into Hawai'ian coastal waters.

Multiple studies have established the use of the four naturally-occurring radium isotopes (^{223}Ra, ^{224}Ra, ^{226}Ra, ^{228}Ra) as tracers of groundwater discharge to coastal systems (e.g., Moore 1996, 2000a, 2003, Charette et al., 2001, Krest and Harvey 2003). Ra isotopes are continually produced in rocks and sediments by U and Th decay. Ra remains largely particle-bound in freshwater, but desorbs from substrate in contact with the brackish to saline waters of unconfined coastal aquifers, giving rise to high-Ra activities in these "subterranean estuaries" relative to seawater (Moore 1999). If other potential Ra sources (rivers, diffusion from sediments) and sinks (radioactive decay) can be constrained, measurements of excess Ra in the coastal ocean can be used to quantify SGD.

Dissolved silica (DSi) is enriched in Hawai'ian groundwater as a result of weathering of the young basaltic bedrock (Visher and Mink 1964; Dollar and Atkinson 1992). Along with depressed salinity, DSi has been used as evidence of groundwater input to the coastal ocean in Hawai'i and other locations (e.g., Garrison et al., 2003, Hwang et al., 2005). However, because Si is a nutrient element subject to biological uptake and cycling, and because new or regenerated DSi may diffuse from bottom sediments to the water column in the absence of advective groundwater discharge, the major controls on DSi distribution must first be established.

The goal of the present study was to expand the existing SGD dataset for the Hawai'ian Islands and quantify groundwater nutrient inputs along the dry leeward shores of the islands, where surface runoff is intermittent, groundwater discharge is the only continuous source of

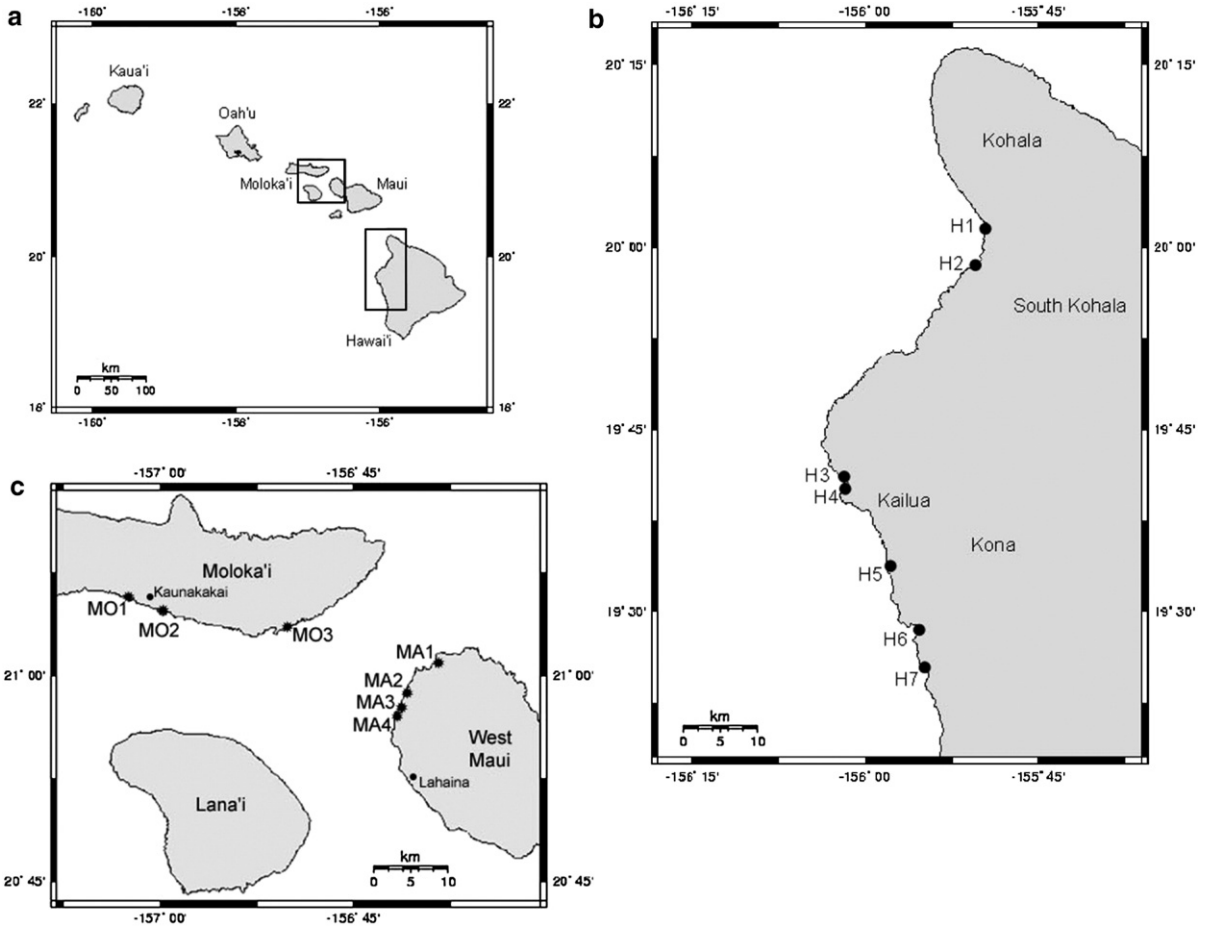

Fig. 1. Map of the main Hawai'ian Islands (a) and the locations of sampling transects along the leeward coasts of Hawai'i (b) and Maui and Moloka'i (c). Site names and numbers are given in Table 1.

terrestrial input to the ocean, and where coastal development is occurring rapidly. We sought to test the use of various geochemical tracers of SGD, particularly radium isotopes, in this environmental setting (dry coast, volcanic island), and to lay the ground work for future, more detailed studies. To these ends we use both short-lived (^{223}Ra and ^{224}Ra) and long-lived (^{226}Ra) radium isotopes, measurements of salinity and DSi concentration and a simple mass balance approach to evaluate the character (in terms of fresh groundwater versus recirculated seawater), magnitude, and nutrient contribution of SGD to coastal waters and fringing reefs at multiple sites along the leeward coasts of Hawai'i, Maui, and Moloka'i.

1.1. Physical setting

Hawai'i (~19.5°N, 155°W), Maui (20.8°N, 156.5°W), and Moloka'i (21°N, 157°W) are three of the eight main islands of the Hawai'ian Islands (Fig. 1). Maui and Moloka'i each consist of two extinct shield volcanoes that formed 0.8–1.9 Ma BP. Hawai'i, the largest and youngest of the islands (0–0.5 Ma BP), is made up of five shield volcanoes. The leeward shorelines of these islands consist of a mixture of low basalt cliffs, intertidal benches and mixed carbonate and basalt sand beaches. The south coast of Moloka'i supports an extensive, nearly continuous fringing coral reef with a shallow (<3 m) reef flat extending more than 1 km offshore to a reef crest dense with coral (Presto et al., 2006). In contrast, fringing reefs on Maui and Hawai'i are discontinuous and of more variable coral cover, with the majority occurring within 1 km of shore in 3–20 m water depth (Storlazzi et al., 2006).

Rainfall on Hawai'i, Maui, and Moloka'i is seasonal, with approximately two to four times as much rain occurring in the winter months (Nov–April) as the summer months (May–Oct) (Shade 1996, 1997; Oki et al., 1999). Orographic uplift associated with the interior mountains traps moisture from the northeast trade winds, restricting rainfall along the leeward (south and west) coasts of all three islands (10 to 100 cm yr^{-1}) (Shade 1996, 1997, Oki et al., 1999). Heavy precipitation in the upland regions of the islands (200–400 cm yr^{-1}) is the primary source of groundwater recharge, supporting seasonal or episodic streamflow in the West Maui and South Moloka'i, where there are a number of well-developed watersheds (Shade 1996, 1997). However, little surface flow reaches the coast during the dry season (Shade 1996). All streams on the leeward coast of Hawai'i are ephemeral and the bulk of the meteoric water reaching the coast at these sites is groundwater in unconfined aquifers flowing through young (0–10 kyr), highly porous basaltic rock (Kay et al., 1977, Oki et al., 1999).

The hydrologic setting at all sites is thought to consist of a brackish/saline coastal aquifer extending inland for a distance that varies from site to site and in response to tidal cycles, seasonal changes in groundwater recharge, bedrock structure and topography (Oki et al., 1999; Lau and Mink 2006). Fig. 2 shows conceptual zonation among saline, brackish, and fresh groundwater in the coastal aquifer. Freshwater occurs only as a thin lens in the upper aquifer, underlain by a layer of active mixing between terrestrial groundwater and intruding seawater (Oki et al., 1999). Because the lava flows and sedimentary deposits that make up these coasts are highly permeable, exchange between the basal aquifer and coastal ocean occurs readily, groundwater

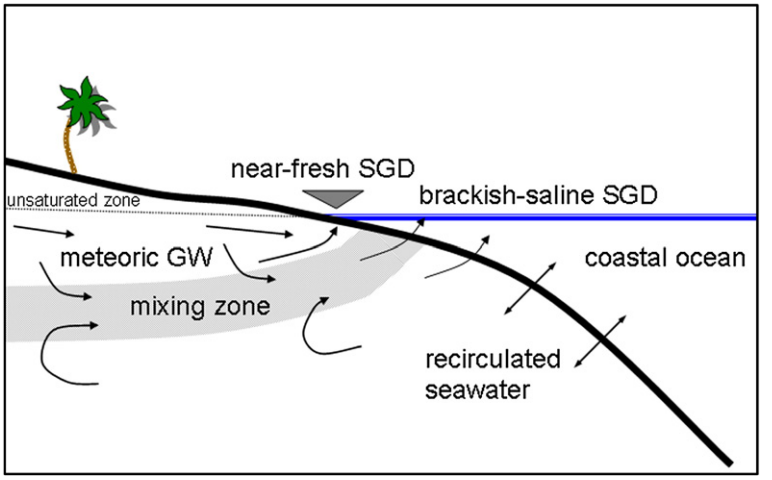

Fig. 2. Conceptual diagram of salinity zonation within the coastal unconfined aquifer at the study sites. The position of the brackish mixing zone ("subterranean estuary") in relation to the shoreline is likely to vary over tidal cycles (e.g., Prieto and Destouni (2005)) and in response to changes in the strength of freshwater discharge (e.g., seasonally).

levels are low (< 1.5 m above sea level), and horizontal head gradients are generally small (Oki et al., 1999), with the possible exception of sites with steep coastal topography (e.g., South Kona sites). Heterogeneity in the structure and porosity of lava flows likely influences the distribution and magnitude of coastal groundwater discharge.

2. Methods and materials

2.1. Study sites and sampling design

Water samples were collected along offshore transects at seven sites on the Kona-Kohala coast of Hawai'i in December 2003 and at four sites along the west coast of Maui and three sites on the southern shore of Moloka'i in July 2003 (Fig. 1). A typical transect consisted of 3–6 sampling points spread between 0 and 75 m offshore – capturing the steepest gradients in tracer and nutrient abundances at these well-mixed sites – along with a sample collected >500 m offshore representing open ocean conditions. Water was collected from the surface layer (0–50 cm depth). On Moloka'i, ten additional single-point samples from the nearshore, back-reef area were collected along a longitudinal transect. Groundwater was collected from springs, pools, wells, or pits dug into the coastal aquifer at most sites. Study sites (listed in Table 1) were selected to encompass a broad geographical area, diverse land-uses adjacent to the coast, and a variety of distinct coastal environments (sandy beach, basalt bench, exposed shores and semi-enclosed bays).

Tidal oscillations are likely to influence the amount of discharge from the coastal aquifer, through the effect of changing water levels on the hydraulic gradient, and its character, via shifts or rearrangements in the positions of the saline, brackish and fresh water zones (Li et al., 1999; Shellenbarger et al., 2006; Robinson et al., 2007). Given the nature of our multi-site survey, it was not possible to control for tidal phase at all sampling locations. Nonetheless, in order to begin to gauge the importance of tidal variability at our sites we collected nearshore samples at Honokohau Beach (H4) on three separate occasions over the course of a tidal cycle.

2.2. Radium isotopes

Water samples (50–100 L) were filtered through columns packed with manganese-coated acrylic fiber (Moore 1976) at flow rates of < 1.5 L min^{-1}. Short-lived Ra isotope activities

Table 1
Sampling site descriptions, control box dimensions and nearshore cross-shore residence time estimates (τ_{xs})

Site ID	Sampling site	Description	Control volume dimensions transect Length/average depth Coast/box type — surface area	τ_{xs} — minimum (based on currents) (min)	τ_{xs} — maximum (based on Ra decay) (d)
H1	Spencer Beach SP Hawai'i	Open bay, sandy beach, sandy bottom	70 m/1.3 m Irregular — 7600 m2 box area	–	2.6
H2	Puako, Hawai'i	Open bay, sandy beach with offshore basalt bench	50 m/0.5 m Straight — 50 × 1 m box	–	1.56
H3	Kaloko, Hawai'i	Open bay, basalt bench	50 m/0.8 m Irregular — 1400 m^2 box area	42	1.56
H4	Honokohau Beach, Hawai'i	Submerged fishpond in open bay; sandy beach	15 m/1 m Irregular — 1375 m^2 box area	–	1.56
H5	Keauhou Bay, Hawai'i	Semi-enclosed bay, sandy bottom	75 m/1.4 m Irregular — 10,600 m^2 box area	–	1.56
H6	Kealekekua Bay, Hawai'i	Open bay, rocky beach	25 m/2.1 m Straight — 25 × 1 m box	–	1.56
H7	Honaunau Bay, Hawai'i	Protected cove, basalt bench	15 m/0.75 m Irregular — 870 m^2 box area	–	1.56
MO1	Kapuaiwa Grove, Molokai	Soft, eroded bank; protected back-reef	60 m/1 m Straight — 60 × 1 m box	50	1.56
MO2	Kamiloloa, Molokai	Soft, eroded bank, protected back-reef	60 m/0.75 m Irregular — 7900 m^2 box area	50	1.56
MO3	Ualapu'e, Molokai	Soft, eroded bank, protected back-reef	60 m/0.61 m Straight — 60 × 150 m box	50	1.56
MA1	Honolua, Maui	Semi-enclosed bay, rocky beach	50 m/1.3 m Irregular — 6200 m^2 box area	–	3
MA2	Kahana, Maui	Open bay, sandy beach	60 m/0.45 m Straight — 60 × 1 m box	40	1.56
MA3	Mahinahina, Maui	Exposed shore, sandy beach	50 m/0.84 m Straight — 50 × 1 m box	–	1.56
MA4	Honokowai, Maui	Exposed shore, sandy beach	45 m/0.5 m Straight — 45 × 1 m box	–	1.56

(^{223}Ra, $t_{1/2}$=11.3 d; ^{224}Ra, $t_{1/2}$=3.66 d) were measured using a scintillation cell interfaced to a photomultiplier and a delayed coincidence counter (Moore and Arnold 1996), and back-corrected for decay since sample collection. The previously reported error for this method is about 10% (Rama et al., 1987; Charette et al., 2001; Moore 2003). Analytical errors based on standard runs for the counting systems used in this study are 6.2% (n=185) and 9.7% (n=142) for ^{224}Ra and ^{223}Ra, respectively. Three to six weeks after sample collection, samples were reanalyzed to correct for ^{228}Th-supported ^{224}Ra activity.

^{226}Ra activity was measured using a RAD7 electronic radon detector (Durridge Co., Bedford MA) according to the method described by Kim et al. (2001). Fibers were moistened with Milli-Q water, placed in air-tight glass tubes, flushed with helium, and incubated for approximately three weeks to allow ^{222}Rn ($t_{1/2}$=3.8 d) to approach secular equilibrium with ^{226}Ra ($t_{1/2}$=1600 yr). Following incubation, samples were attached to the RAD7 in a closed loop and analyzed for 4–7 hr. ^{226}Ra activity was measured as the decays per minute of ^{218}Po ($t_{1/2}$=3.05 min), the daughter of ^{222}Rn, in secular equilibrium with both ^{222}Rn and ^{226}Ra, with an efficiency of about 10%. The analytical error (based on standard runs) for the detector used in this study is 10.5% (n=30). Triplicate measurements of 16 random samples indicated that on average our measurement error was 8.8%.

2.3. Nutrients, salinity, and temperature

Sub-samples for nutrient analyses were filtered through 0.2 μm or 0.45 μm filters into triple-rinsed, acid-cleaned, 30 ml polyethylene bottles and kept frozen until analysis. Nitrate plus nitrite, nitrite, ammonium, soluble reactive silica (DSi) and soluble reactive phosphorus (SRP) were analyzed using colorimetric methods on a 5-channel, hybrid continuous flow analyzer at Oregon State University. Technicon AutoAnalyzer II™ components were used to measure phosphate and ammonium; Alpkem RFA 300™ components were used for silicic acid, nitrate plus nitrite, and nitrite. Water temperature and salinity for each sample were determined in the field using a handheld YSI probe (model 30, Yellow Springs, OH).

2.4. Mass balance models and flux calculations

Groundwater discharge at each site was estimated using measured tracer abundances (Ra isotopes, DSi, and/or salinity) and a simple mass balance model adapted from Moore (1996). This model was applied to a nearshore control volume or "box", the dimensions of which depended on the shape of the coastline at a given site. At sites where the coastline was approximately linear on the scale of the sampling regime (H2, H6, MA2, MA3, MA4, MO1, MO3), we defined a rectangular box encompassing the transect. Because our sampling scheme does not account for alongshore variability at a single location, the alongshore length of these "straight boxes" can be assigned as 1 m. The exception to this rule was at Ualapu'e (MO3), where the larger number of samples allowed for greater alongshore box dimensions. At other sampling sites situated within embayments or on otherwise irregular coastlines (H1, H3, H4, H5, H7, MA1, MO2), larger boxes were defined to encompass the sampling transect and all shoreline points within one transect length of the most seaward nearshore sample. Water depths within each box were based on measurements at each sampling point.

Nearshore tracer abundances (average of all samples within the box) were assumed to be supported by the contributions of SGD and offshore seawater, represented by water sampled from the unconfined surficial aquifer and the open ocean, respectively. Surface runoff was absent at all sites at the time of sampling, and thus was eliminated from the mass balance. Diffusive fluxes of Ra and DSi from bottom sediments were not differentiated, and were assumed to be small relative to advective fluxes (see Section 3.4.2). With these constraints, the amount of groundwater input needed to balance the excess of a conservative tracer in the coastal control volume was calculated as follows:

$$\frac{\left(\overline{A}_{ns} - A_{off}\right)V_{box}}{\tau A_{gw}} = Q_{gw} \tag{1}$$

where A_{ns}, A_{off}, and A_{gw} represent the tracer activities or concentrations (dpm 100 L^{-1} for Ra; μmol L^{-1} for DSi) in the nearshore, offshore water, and groundwater end-member, respectively, τ is the cross-shore water exchange time in the box, V is the box volume (m^3), and Q_{gw} is the balance of groundwater input to the box. This calculation yields an estimate of SGD in m^3 d^{-1}. Salinity balance calculations take a very similar form:

$$\frac{f\mathrm{FW}_{ns}V_{box}}{\tau f\mathrm{FW}_{gw}} = Q_{gw} \tag{2}$$

where fFW$_{ns}$ and fFW$_{gw}$ are the freshwater fractions of the nearshore box and groundwater end-member, calculated as the difference between the offshore salinity and the average salinity in the box, normalized to the offshore salinity. In this calculation we neglect freshwater inputs other than groundwater (e.g., stream input, precipitation) and loss processes (e.g., evaporation).

Radioactive decay of the short-lived isotopes ^{223}Ra and ^{224}Ra can be included in the mass balance with a slight modification:

$$\left(\left(\overline{A}_{ns} - A_{off}\right)V_{box}\left(\lambda_{Ra} + \frac{1}{\tau}\right)\right)\frac{1}{A_{gw}} = Q_{gw} \tag{3}$$

where λ_{Ra} is the decay constant of the Ra isotope in question (λ_{223}=0.0608 d^{-1}; λ_{224}=0.1893 d^{-1}).

The above mass balance calculations assume simple mixing between offshore seawater and a single, uniform groundwater source. At several sites, where distinct near-fresh and saline groundwater sources were identified, the mass balance was modified to account for three end-members, and required two tracers to solve for the two unknowns. For example, the system of mass balance equations for a short-lived Ra isotope tracer

$$\left(\left(\overline{A}_{ns} - A_{off}\right)V_{Box}\left(\lambda_{Ra} + \frac{1}{\tau}\right)\right) = A_{sgw}Q_{sgw} + A_{fgw}Q_{fgw} \tag{4a}$$

and DSi tracer

$$\frac{\left(\overline{A}_{ns} - A_{off}\right)V_{Box}}{\tau} = A_{sgw}Q_{sgw} + A_{fgw}Q_{fgw} \tag{4b}$$

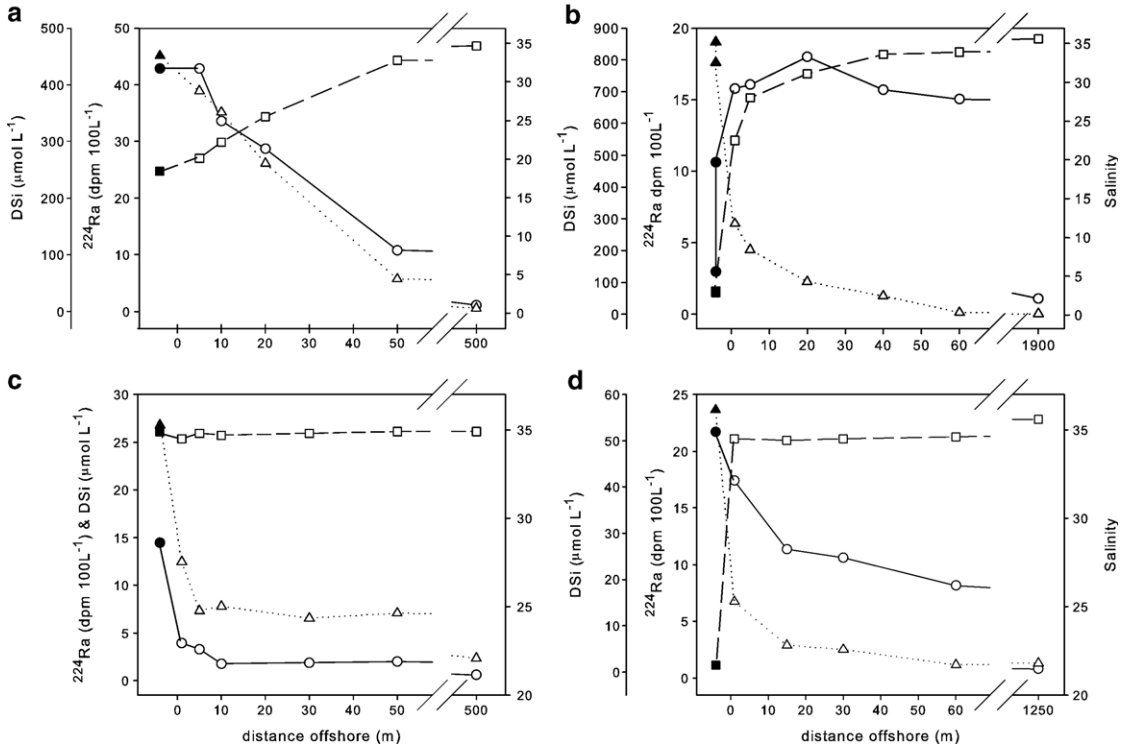

Fig. 3. Offshore gradients in tracer abundances for representative sampling locations: (a) Kaloko (H3), Hawai'i; (b) Kapuaiwa Grove (MO1), Moloka'i; (c) Puako Bay (H2), Hawai'i; (d) Kahana (MA3), Maui. ^{224}Ra (○), DSi (△) and salinity (□) shown; groundwater samples indicated by solid shapes.

can be solved to yield separate estimates of saline groundwater (Q_{sgw}) and near-fresh groundwater (Q_{fgw}) input to the coastal zone.

These site-specific SGD estimates ($m^3\ d^{-1}$) were converted to fluxes ($m^3\ m^{-2}\ d^{-1}$) by normalizing to a seepage face assumed to consist of the entire seafloor area (SA) of the nearshore box. Though previous work suggests that fresh SGD is generally concentrated near the low tide mark (Robinson et al., 2007), extensive offshore SGD has been observed at other Hawai'ian sites (Garrison et al., 2003). Since the actual extent of the seepage faces at our sites is unknown, we have adopted a conservative approach. Additions of DIN, SRP, and DSi to the nearshore zone were estimated by multiplying the respective groundwater end-member concentrations by the calculated SGD flux.

2.5. Nearshore mixing times

Nearshore water residence times at our study sites are a complex function of wind-, wave-, and tidally-driven circulation, and are likely to vary considerably in response to changing conditions. Based on multi-year measurements of current velocities on the Moloka'i reef flat at a point near our Kamiloloa (MO2) sampling site, Presto et al. (2006) identified two seasons (trade-wind versus non-trade-wind) with at least four distinct circulation regimes. During the summer "trade-wind" conditions that best match the conditions during our July 2003 sampling, the mean current was to the west-southwest, with a slight, 2 cm/s offshore component, regardless of tidal cycle (Presto et al., 2006). Similar work off West Maui has shown that the dominant mode of transport on this coast is alongshore, with only a small cross-shore component (Storlazzi et al., 2003). A more detailed study off of Kahana (MA2) highlights the importance of the tides in driving this alongshore flow, but also detected cross-shore currents during trade-wind conditions with a range in offshore velocities of about −10 to 10 cm/s, with a more typical value of 2.5 cm/s (Storlazzi and Jaffe 2003). Mean net flow off of Kaloko (H3) appears to be similar (~2.8 cm/s, NW) (C. Storlazzi, pers. comm.). We estimate the maximum cross-shore component of this vector relative to the sampling transect to be approximately 2 cm/s. It is important to note that these current measurements were made in deeper water well offshore of our transects (>50 m offshore) and probably overestimate current velocities within our coastal boxes.

Based on these average cross-shore current velocities, we calculate τ, the cross-shore residence time for the nearshore box, as the amount of time for a parcel of water to traverse the entire length of the sampling transect. These current-based residence times, considered minimum estimates, are given in Table 1. SGD and nutrient flux estimates generated using current-based residence times are almost certainly overestimates.

Moore (2000b) suggested a simple, independent approach to assessing nearshore exchange times derived from cross-shore profiles of the activity ratio of ^{224}Ra to ^{223}Ra:

$$\left(\frac{^{224}\mathrm{Ra}}{^{223}\mathrm{Ra}}\right)_{\mathrm{nr}} = \left(\frac{^{224}\mathrm{Ra}}{^{223}\mathrm{Ra}}\right)_{i} \left(\frac{e^{-\lambda 224 t}}{e^{-\lambda 223 t}}\right) \quad (5)$$

where Ra_i represents the end-member Ra activity, Ra_{nr} is the Ra activity at a given distance offshore, and λ_{223} and λ_{224} are the decay constants of ^{223}Ra and ^{224}Ra. Because ^{224}Ra decays at a faster rate than ^{223}Ra, their activity ratio will decrease with time following an initial Ra enrichment and subsequent isolation from the source. This model assumes that there is a single, constant activity ratio for the source end-member, that the open ocean contains negligible ^{223}Ra and ^{224}Ra, and that no additions or losses of Ra occur other than mixing and radioactive decay. We have applied this model as an additional method of estimating nearshore exchange times. The sensitivity of this approach, however, is limited by the accuracy of the radium isotope measurements. Assuming measurement errors of 10% for both isotopes, changes in the ratio of ^{224}Ra:^{223}Ra of coastal water will only become detectable 1.56 days after isolation from the radium source. At most of our sites, little or no decay of ^{224}Ra relative to ^{223}Ra was detectable within our measurement error, supporting the conclusion that nearshore residence times are short. For these sites, the theoretical time of detectability (1.56 d) is considered a maximum estimate of the residence time (Table 1) and will produce conservative flux estimates for SGD and associated solutes.

3. Results and discussion

3.1. General patterns

Submarine groundwater discharge was identified at all sites sampled. At certain sites, notably Spencer Beach Park (H1), Kaloko Fishpond (H3), and Honokohau Beach (H4) on Hawai'i, and Kapuaiwa Grove (MO-1) and Kamiloloa (MO-2) on Molokai, groundwater discharged visibly from intertidal springs or as small rivulets and intertidal rills in the sand within a few meters of the water's edge at low tide, while at other sites the SGD was recognized by lowered salinity or tracer enrichments. Tracer abundances (Ra, DSi) and the degree of freshening were typically greatest within ten meters of the water line, declining toward seawater values within 100 m offshore (Fig. 3a–d). These offshore gradients were often matched by gradients in inorganic nitrogen and phosphorus (see Tables 2a, 2b, 2c). Taken together, the observed patterns are consistent with terrestrial sources of freshwater, Ra, and associated nutrients, most likely through submarine groundwater discharge.

3.1.1. Tracers in groundwater, nearshore and offshore water

^{223}Ra and ^{224}Ra activities in groundwater samples from the unconfined coastal aquifer were highly variable, ranging from 0.08–6.11 dpm 100 L^{-1} ^{223}Ra and 1.29–55.71 dpm 100 L^{-1} ^{224}Ra. With the exception of low salinity groundwater, which usually contained low Ra activities, short-lived Ra was typically 2 to 10 times more abundant in groundwater than in nearshore samples. Nearshore activities of short-lived Ra spanned a similarly wide range (0.04–2.77 dpm 100 L^{-1} ^{223}Ra; 1.32–42.86 dpm 100 L^{-1} ^{224}Ra), generally mirroring adjacent groundwater samples and declining with distance offshore. In contrast, groundwater and nearshore ^{226}Ra activities were enriched above the seawater background at only a handful of sites (H1, H3, H4, MO2, MA1, MA2). ^{223}Ra and ^{224}Ra activities in samples of all types were generally well-correlated on a site-by-site basis (Fig. 4a and b). Differences in the slope of this relationship may result from different activities of Ra precursors in aquifer rocks or varying groundwater recharge rates and aquifer residence times (Moore 2003). The linear relationship between the two short-lived isotopes in coastal zone samples at most sites indicates that ^{224}Ra:^{223}Ra ratios were constant (within our measurement error) and nearshore residence times less than 1.56 days. The greater degree of scatter observed at Molokai locations is probably due to additional Ra inputs within the nearshore zone, away from shore, meaning that our estimates of nearshore residence time are less robust for these sites (MO1, MO2, MO3). Detectable declines in the ^{224}Ra:^{223}Ra ratio within the nearshore box occurred only at Honolua Bay (MA1) and Spencer Beach (H1), both of which were sampled in calm conditions (Table 1).

Groundwater salinity ranged from 0.5 in the freshwater pond at Ualapu'e, Moloka'i (MO3) to values indistinguishable from seawater (>34.5) at Puako Bay (H2) and Honokowai (MA4). Nearshore salinities ranged from 20–34 at sites experiencing strong discharge of groundwater with a meteoric component (H1, H3, H4, H5, H6, H7; all Molokai sites), increasing with distance offshore. At other sites (H2, all Maui sites), salinities were similar to offshore seawater (34.5–35.5). DSi concentrations were negatively correlated with salinity ($R^2=0.93$, $p<0.001$, $n=79$) in groundwater, nearshore, and offshore samples from all Hawai'i and Molokai sites; a strong relationship was also observed on Maui ($R^2=0.80$, $p<0.001$, $n=25$), though with a different slope (Fig. 5a and b). The strength of these relationships indicates that dilution is the dominant control on the distribution of silica at these sites, and that DSi can be used locally as a tracer of SGD.

The nine samples collected in this study from >300 m offshore were geochemically uniform, with low Ra activities (0.08±0.02 dpm 100 L^{-1} ^{223}Ra; 0.97±0.42 dpm 100 L^{-1} ^{224}Ra; 6.40±0.22 dpm 100 L^{-1} ^{226}Ra) and DSi concentrations (3.3±2.5 μmol L^{-1}). Salinity offshore of Maui and Molokai (35.3–35.6) was slightly higher than off of Hawai'i (34.7–34.9), perhaps reflecting seasonal differences in evaporation or stronger freshwater input along the Kona coast.

3.1.2. Nearshore mixing and site characterization

The summary in §3.1.1 conceals patterns between sites and among the various tracers used that require further explication. Fig. 6 shows mixing diagrams of ^{224}Ra and salinity measured at each sampling site. Observed patterns at half of the sites (H2, H3, H4, H7, MA3, MA4, MO2) are consistent with simple mixing between offshore water and a relatively uniform groundwater end-member (Fig. 6a and b). At the remaining seven sites (H1, H5, H6, MA1, MA2, MO1, MO3), nearshore activities of ^{224}Ra falling above the expected mixing line (Fig. 6b, c, d and e) are indicative of additional sources of radium — potentially SGD of a different character. Based on these mixing diagrams, and on the geochemical character of sampled groundwater, the 14 transect sites comprising this study can be grouped into 3 general categories (Fig. 7):

- *Category 1*: Low salinity (1–12), high DSi (300–850 μmol L^{-1}) groundwater with suppressed Ra activities (0.08–0.3 dpm

Table 2a
Results from Kona-Kohala (Hawai'i) transects

Site	Lat. °N	Long. °W	Sample (m)	Collection date	Tide [a] (level)	Temp °C	Salinity	(dpm 100 L^{-1})			(μmol L^{-1})			
								^{223}Ra	^{224}Ra	^{226}Ra	[DSi]	[DIN]	[SRP]	N:P
H1 *Spencer Beach Park*	20° 1.450′	155° 49.353′	GW (spr.)	16-Dec-03	Low (0.1)[#]	29.1	2.9	0.26	6.6	1.9	798	47.1	1.22	38.5
			GW (pit)	16-Dec-03	Low	25.2	32.2	1.09	11.2	7.2	80.8	12.5	0.73	17.1
			1	16-Dec-03	Low	27.0	27.2	0.22	4.52	5.05	202	16.3	0.46	35.4
			5	16-Dec-03	Low	26.9	31.0	0.27	3.64	5.91	150	12.4	0.39	31.8
			15	16-Dec-03	Low	26.0	30.5	0.10	2.26	5.68	30.4	2.86	0.26	11.0
			70	16-Dec-03	Ebb (0.5)	25.8	30.9	0.24	2.12	6.17	6.06	1.02	0.17	6.0
			500	16-Dec-03		25.8	31.2	0.06	1.03	6.45	3.70	0.91	0.19	4.8
H2 *Puako Bay*	19° 58.409′	155° 50.300′	GW (pit)	16-Dec-03	High (0.55)[#]	26.4	34.9	1.28	14.6	6.99	26.8	7.1	0.96	7.4
			1	16-Dec-03	High	25.3	34.5	0.33	4.04	6.09	12.4	1.5	0.22	6.8
			5	16-Dec-03	High	25.8	34.8	0.11	3.44	6.55	7.3	0.51	0.16	3.2
			10	16-Dec-03	High	26.1	34.7	0.13	1.86	6.31	7.8	0.81	0.17	4.8
			30	16-Dec-03	High	26.8	34.8	0.04	1.97	5.60	6.5	0.72	0.17	4.2
			50	16-Dec-03	High	26.2	34.9	0.12	2.08	6.41	7.1	0.79	0.13	6.1
			1000	16-Dec-03	–	25.8	34.9	BD	0.60	6.07	1.2	0.33	0.16	2.1
H3 *Kaloko Fishpond*	19° 41.215′	156° 1.973′	GW (spr.)	15-Dec-03	Low (0.1)[+]	19.5	18.4	3.53	42.86	9.71	451	44.7	2.68	16.7
			5	15-Dec-03	Low	20.9	20.1	2.67	42.86	8.43	389	39.0	2.36	16.5
			10	15-Dec-03	Low	22.7	22.2	2.77	33.62	7.66	351	32.5	2.06	15.8
			20	15-Dec-03	Low	23.1	25.5	2.56	28.69	8.61	261	24.7	1.63	15.2
			50	15-Dec-03	Low	25.6	32.8	0.97	10.80	7.82	57.5	5.5	0.49	11.2
	19° 40.343′	156° 1.841′	500	18-Dec-03	Flood (0.4)	25.9	34.7	0.08	1.12	6.14	5.75	0.71	0.19	3.7
H4 *Honokohau Beach*	19° 40.261′	156° 1.572′	GW (pond)	17-Dec-03	Ebb (0.45)[+]	24.7	13.5	5.26	45.05	8.33	502	49.0	2.46	19.9
			1	17-Dec-03	Ebb	24.7	31.2	1.28	12.89	7.59	92.9	8.23	0.74	11.1
			7.5	17-Dec-03	Ebb	24.7	31.5	1.04	14.38	7.22	86.0	7.19	0.70	10.3
			15	17-Dec-03	Ebb	24.9	32.5	1.00	12.46	7.37	70.8	5.46	0.54	10.1
			1	17-Dec-03	Low (0.1)	23.3	20.9	2.93	30.66	8.50	367	33.3	2.11	15.8
			5	17-Dec-03	Low	22.7	19.9	2.34	41.37	6.73	400	44.1	2.16	20.4
			15	17-Dec-03	Low	23.0	24.2	3.40	34.24	8.28	234	23.3	1.34	17.4

			GW (pond)	18-Dec-03	Flood (0.4)[+]	21.9	13.6	6.11	55.71	8.90	524	58.1	2.67	21.7
			1	18-Dec-03	Flood	23.9	29.2	1.54	18.54	8.45	131	12.5	0.93	13.4
			5	18-Dec-03	Flood	24.4	31.3	1.07	16.58	7.80	117	9.99	0.79	12.6
			15	18-Dec-03	Flood	24.6	32.4	0.65	8.99	7.17	51.6	3.20	0.38	8.4
	19° 40.252′	156° 1.708′	200	18-Dec-03	Flood (0.4)	25.3	34.2	0.21	2.09	–	22.9	1.55	0.20	7.8
	19° 40.343′	156° 1.841′	500	18-Dec-03	Flood (0.4)	25.9	34.7	0.08	1.12	6.14	5.75	0.71	0.19	3.7
Site	Lat. °N	Long. °W	Sample (m)	Collection date	Tide[b] (level)	Temp °C	Salinity	(dpm 100 L^{-1})			(μmol L^{-1})			
								^{223}Ra	^{224}Ra	^{226}Ra	[DSi]	[DIN]	[SRP]	N:P
Kaloko-Honokohau NP	19° 40.975′	156° 1.971′	GW-fed pond	17-Dec-03	High (0.5)[+]	20.7	14.2	3.47	39.60	8.61	523	66.7	3.24	20.6
(other sites)	19° 40.956′	156° 1.952′	GW-fed pond	17-Dec-03	High (0.5)	21.0	13.7	4.22	36.73	8.11	432	41.0	2.18	18.8
	19° 41.820′	156° 1.978′	shore spring	17-Dec-03	High (0.5)	19.4	13.2	2.57	27.89	5.74	547	45.3	2.55	17.8
	19° 40.661′	156° 1.479′	inland spring	18-Dec-03	High (0.5)	24.4	11.9	0.46	7.97	7.03	544	53.0	4.09	13.0
	19° 40.468′	156° 1.577′	shore spring	17-Dec-03	Ebb (0.2)	22.0	15.1	3.41	41.57	6.86	498	46.2	2.58	17.9
H5 *Keauhou Bay*	19° 33.272′	155° 57.723′	GW (pit)	(see note)[#]	Low		10.5	0.24	2.64	–	624	174	4.08	42.8
			1 m	20-Dec-03	Low (0.2)[♣]	24.2	22.5	0.75	8.91	6.15	316	61.3	2.25	27.2
			5 m	20-Dec-03	Low	25.5	31.2	0.94	4.54	6.85	85.7	20.6	0.70	29.4
			75 m	20-Dec-03	Low	25.7	33.4	0.27	4.16	6.58	70.0	15.7	0.79	19.9
	19° 33.569′	155° 58.271′	1000 m	20-Dec-03	Low	26.1	34.7	BD	0.38	6.66	1.13	0.72	0.18	4.0
H6 *Kealakekua Bay*	19° 28.427′	155° 55.172′	GW (pit)	20-Dec-03	Flood (0.3)[♣]	24.3	11.6	0.15	2.30	4.57	308	37.0	0.96	38.5
			1 m	20-Dec-03	Flood	26.0	33.3	0.43	1.94	7.24	38.3	4.55	0.37	12.3
			5 m	20-Dec-03	Flood	26.1	33.8	0.19	2.18	6.53	21.8	2.01	0.26	7.7
			10 m	20-Dec-03	Flood	26.1	33.6	0.12	1.81	6.75	17.2	1.87	0.26	7.2
			25 m	20-Dec-03	Flood	26.1	34.1	0.07	1.86	6.91	19.7	2.18	0.28	7.8
	19° 33.569′	155° 58.271′	1000 m	20-Dec-03	Low	26.1	34.7	BD	0.38	6.66	1.13	0.72	0.18	4.0
H7 *Honaunau Bay*	19° 25.271′	155° 54.689′	GW (pond)	20-Dec-03	Ebb (0.35)[♣]	27.8	12.7	0.80	10.03	3.44	596	17.0	2.49	6.8
	19° 24.347′	155° 54.643	1 m	20-Dec-03	Ebb	25.1	22.4	0.36	4.86	5.03	309	25.4	1.80	14.1
			7.5 m	20-Dec-03	Ebb	25.9	26.6	0.29	4.17	6.53	204	16.1	1.24	13.0
			15 m	20-Dec-03	Ebb	26.0	28.1	0.27	4.36	7.11	176	14.2	1.10	12.9
			100 m	20-Dec-03	Ebb	26.7	33.9	0.22	1.21	–	17.1	1.58	0.28	5.6
	19° 33.569′	155° 58.271′	1000 m	20-Dec-03	Low	26.1	34.7	BD	0.38	6.66	1.13	0.72	0.18	4.0

[a] Tide water levels in meters above mean low low water (MLLW); data from NOAA stations at: [#] Kawaihae; [+] Hilo, adjusted for Kailua-Kona.

[b] Tide water levels in meters above mean low low water (MLLW); Data from NOAA stations at: [+] Hilo, adjusted for Kailua-Kona; [♣]Hilo, adjusted for Napoopoo. [#] Keauhou Bay groundwater values are the average of samples collected on 30 March 2005, and 6 April 2006, at low tide.

Table 2b
Results from Moloka'i transects

Site	Lat. °N	Long. °W	Sample	Collection date	Tide[a] (level)	Temp °C	Salinity	(dpm 100 L^{-1})			(μmol L^{-1})			
								^{223}Ra	^{224}Ra	^{226}Ra	[DSi]	[DIN]	[SRP]	N:P
MO1 *Kapuaiwa Grove*	21° 5.760′	157° 2.320′	GW spr. #1	10-Jul-03	Flood (0.25)†	24.6	2.9	0.25	2.98	2.52	791	60.3	2.01	30.8
	21° 5.766′	157° 2.370′	GW spr. #2	13-Jul-03	Low (−0.08)	24.4	3.1	0.70	10.61	2.16	856	67.0	2.37	28.3
	21° 5.764′	157° 2.333′	1 m	10-Jul-03	Flood (0.37)	27.0	22.5	1.95	15.78	4.57	285	22.8	1.38	16.5
			5 m	10-Jul-03	Flood (0.44)	27.4	28.0	1.02	16.05	5.28	203	13.1	0.81	16.2
			20 m	10-Jul-03	Flood (0.58)	27.7	31.1	0.60	18.00	5.71	102	3.14	1.09	2.9
			40 m	10-Jul-03	High (0.66)	27.7	33.6	0.90	15.69	6.88	57.6	1.43	0.13	11.0
			60 m	10-Jul-03	High (0.77)	27.8	33.9	0.34	15.03	6.48	5.74	0.50	0.13	3.8
MO2 *Kamiloloa*	21° 4.712′	156°59.810′	GW	10-Jul-03	Ebb (0.51)†	26.5	33.4	2.05	46.96	10.05	46.5	3.88	0.89	4.4
			5 m	10-Jul-03	Ebb (0.37)	26.9	34.3	0.70	25.84	6.41	26.8	2.62	0.02	131
			20 m	10-Jul-03	Ebb (0.32)	27.4	34.5	1.73	28.48	8.08	20.2	1.39	–	–
			60 m	10-Jul-03	Ebb (0.26)	26.9	35.2	1.10	23.77	8.25	9.89	1.37	0.11	12.5
MO3 *Ualapu'e*	21° 3.392′	156°50.061′	GW (pond)	11-Jul-03	Flood (0.8)‡	24.2	0.5	0.08	1.29	6.04	593	8.35	4.03	2.1
	21° 3.492′	156°49.995′	1 m (east)	11-Jul-03	Flood (0.0)	25.3	22.4	0.58	11.15	5.34	207	2.80	1.60	1.8
			15 m (east)	11-Jul-03	Flood (0.1)	26.0	31.3	0.47	8.09	6.37	63.2	0.99	0.75	1.3
	21° 3.391′	156°50.059′	1 m (cen.)	11-Jul-03	Flood (0.75)	28.1	32.2	0.25	11.84	6.30	52.0	3.97	0.92	4.3
			20 m (cen.)	11-Jul-03	Flood (0.5)	27.6	32.6	0.49	7.17	7.11	42.8	1.25	0.74	1.7
	21° 3.375′	156°50.067′	1 m (west)	11-Jul-03	Flood (0.2)	28.2	27.6	0.82	12.85	6.90	112	3.71	1.52	2.4
			10 m (west)	11-Jul-03	Flood (0.3)	26.5	32.1	0.79	9.62	5.61	50.8	1.40	0.66	2.1
			60 m (cen.)	11-Jul-03	Flood (0.6)	27.5	34.2	0.35	5.38	5.59	17.5	1.08	0.12	9.0
Offshore (beyond reef break)	21° 4.764′	157° 2.681′	1.9 km	10-Jul-03	–	26.2	35.6	0.09	1.10	6.60	1.49	1.36	0.72	1.9
Alongshore study — 1 m offshore														
Ualapu'e	21° 3.497′	156°49.989′	1 m	12-Jul-03	Flood (0.4)‡	27.3	29.8	0.48	9.42	6.51	92.2	2.69	0.88	3.1
Kilohana	21° 3.404′	156°50.051′		12-Jul-03	Flood (0.3)‡	28.4	27.7	0.54	15.64	6.03	118	0.60	1.29	0.5
Mile mark 12	21° 3.447′	156°51.083′		12-Jul-03	Flood (0.25)‡	25.8	28.7	0.36	7.77	6.40	129	0.93	1.16	0.8
Mile mark 8–9	21° 3.315′	156°53.665′		12-Jul-03	Flood (0.15)‡	28.1	30.6	1.03	31.51	9.87	118	6.68	1.24	5.4
Kakahai'a Park	21° 3.744′	156°56.370′		12-Jul-03	Flood (0.0)†	26.3	32.7	0.47	28.22	8.19	54.3	3.76	0.96	3.9
Mile mark 4–5	21° 3.984′	156°57.366′		12-Jul-03	Flood (−0.03)†	28.6	34.7	0.91	34.50	9.13	37.3	7.00	0.71	9.9
One Ali'i Park	21° 4.236′	156°58.547′		12-Jul-03	Flood (−0.1)†	27.3	27.3	0.52	32.37	7.93	91.9	2.94	1.09	2.7
Kamiloloa	21° 4.692′	156°59.808′		13-Jul-03	Flood (0.16)†	31.4	32.1	0.87	30.54	8.47	44.8	1.63	0.64	2.5
Kaunakakai	21° 5.136′	157° 1.278′		13-Jul-03	Flood (0.05)†	33.5	32.6	1.41	31.06	9.20	70.7	4.26	1.04	4.1
Malama Park	21° 5.235′	157° 1.493′		13-Jul-03	Flood (−0.03)†	29.7	(35.9)	2.52	35.62	10.34	47.4	2.19	0.55	4.0

[a]Tide water levels in meters above mean low low water (MLLW); from NOAA Honolulu station, adjusted for: † Kaunakakai or ‡ Kamalo.

Table 2c
Results from Maui transects

Site	Lat. °N	Long. °W	Sample	Collection date	Tide (level)	Temp °C	Salinity	(dpm 100 L^{-1})			(μmol L^{-1})			
								^{223}Ra	^{224}Ra	^{226}Ra	[DSi]	[DIN]	[SRP]	N:P
MA1 *Honolua Bay*	21° 0.766′	156° 38.311′	GW (pond)	7-Jul-03	High (0.45)	27.0	16.3	0.64	29.64	16.37	45.5	3.26	0.44	7.4
			1 m	7-Jul-03	High	26.7	34.8	–	–	6.89	9.74	1.71	0.09	19.0
			15 m	7-Jul-03	Ebb (0.4)	26.6	35.0	0.07	2.16	5.69	4.23	1.81	0.11	16.5
			50 m	7-Jul-03	Ebb	26.3	35.0	0.07	1.32	5.45	8.53	1.79	0.69	2.6
			130 m	7-Jul-03	Ebb	25.8	35.4	0.01	1.32	6.18	5.64			
			1.25 km	7-Jul-03	High	25.4	35.3	0.05	0.80	6.57	1.84	1.00	0.15	6.7
MA2 *Kahana*	20° 58.648′	156° 40.648′	GW (pond)	4-Jul-03	High (0.3)	24.2	21.7	0.81	21.71	21.85	56.7	33.5	0.82	41.1
			1 m	6-Jul-03	High (0.4)	23.8	34.5	0.59	17.41	9.35	15.2	1.87	0.67	2.8
			15 m	6-Jul-03	High	25.4	34.4	0.53	11.36	6.75	5.75	2.22	0.60	3.7
			30 m	6-Jul-03	High	25.0	34.5	0.54	10.61	7.30	4.85	1.44	0.65	2.2
			60 m	6-Jul-03	High	25.7	34.6	0.30	8.16	9.04	1.52	1.52	0.70	2.2
			350 m	7-Jul-03	Flood (0.4)	25.3	35.5	0.06	1.51	6.35	3.87	1.85	0.65	2.8
MA3 *Mahinahina*	20°57.612′	156°41.063′	GW (pit)	4-Jul-03	Low (0.1)	26.6	31.5	1.04	14.01	6.51	42.4	185	3.34	55.4
			1 m	6-Jul-03	Low (0.3)	26.1	34.2	0.45	3.52	6.19	12.7	1.73	–	–
			15 m	6-Jul-03	Low	26.9	34.0	0.21	3.36	7.86	17.5	6.88	–	–
			30 m	6-Jul-03	Low	26.8	33.9	0.21	2.64	7.00	27.9	8.01	0.50	16.0
			50 m	6-Jul-03	Low	26.7	34.2	0.23	3.11	6.53	24.3	8.21	0.62	13.2
			350 m	7-Jul-03	Flood (0.4)	25.4	35.3	0.08	1.59	6.57	8.36	2.67	0.69	3.9
MA4 *Honokowai*	20°57.032′	156°41.428′	GW (pit)	3-Jul-03	Flood (0.2)	25.8	34.5	0.91	10.71	6.96	11.1	21.6	0.63	34.3
			1 m	5-Jul-03	Flood (0.3)	27.2	34.9	0.42	4.71	6.72	5.55	1.18	0.26	4.5
			15 m	5-Jul-03	Flood (0.4)	27.4	35.1	0.30	4.48	6.12	2.72	1.16	0.13	8.9
			45 m	5-Jul-03	Flood (0.4)	27.4	35.3	0.42	4.70	6.86	2.90	1.96	0.64	3.1
			400 m	5-Jul-03	Ebb (0.3)	25.7	35.2	0.11	0.58	6.17	2.19	1.08	0.13	8.3

Tide water levels in meters above mean low low water (MLLW); from NOAA Kahului station, adjusted for Lahaina.

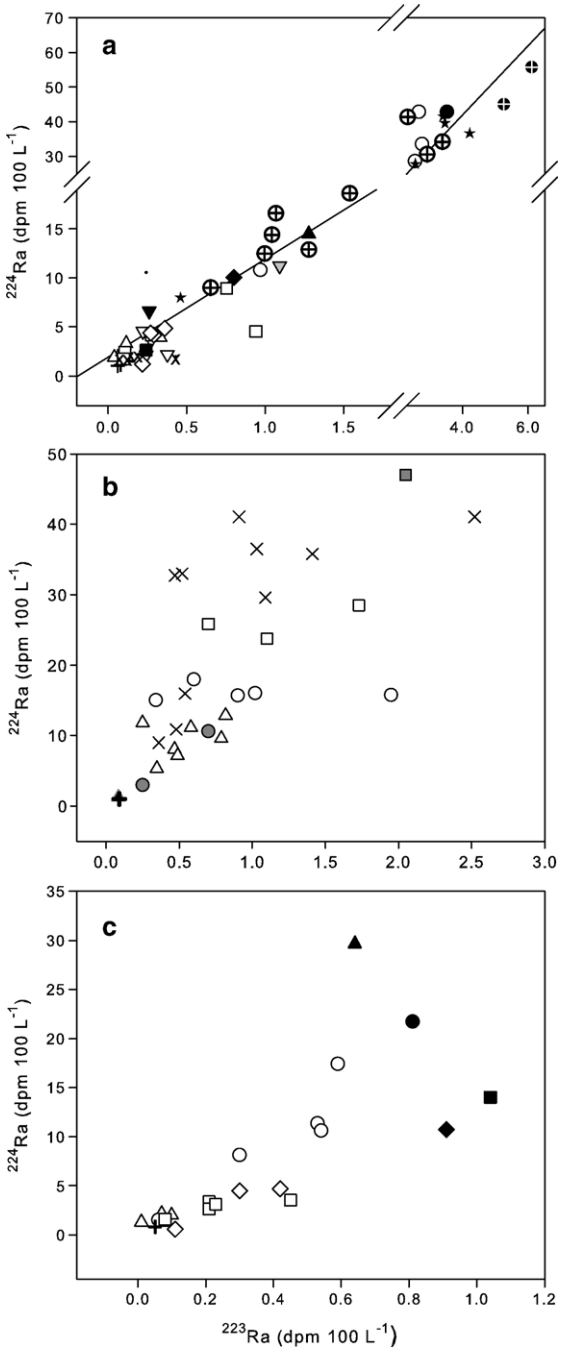

Fig. 4. Correlation between ^{224}Ra and ^{223}Ra activities at all sampling locations. Groundwater samples denoted as solid shapes; coastal zone samples by open shapes. Offshore samples given as (+). (a) Strong correlation (R^2=0.92, n=50) at all Big Island sites: H1 (▽), H2 (△), H3 (○), H4 (⊕), H5 (□), H6 (X), H7 (◇) and groundwater within Kaloko-Honokohau National Park (★). (b) All Moloka'i locations (R^2=0.47, n=30); site-specific correlation coefficients in parenthesis: MO1 (○, 0.60, n=8), MO2 (□, 0.79, n=4), MO3 (△, 0.68, n=8) and alongshore samples (X, 1 m off shore, 0.62, n=10). (c) All Maui locations (R^2=0.73, n=23); site-specific correlation coefficients in parenthesis: MA1 (△, 0.99, n=7), MA2 (○, 0.96, n=6), MA3 (□, 0.97, n=6), MA4 (◇, 0.98, n=5).

100 L^{-1} ^{223}Ra; 1–7 dpm 100 L^{-1} ^{224}Ra; 1–5 dpm 100 L^{-1} ^{226}Ra); *Sites*: Spencer Beach (H1), Keauhou Bay (H5), Kealekekua Bay (H6), Hawai'i; Kapuaiwa Grove (MO1) and Ualapu'e (MO3), Moloka'i.

- *Category 2*: Intermediate salinity (13–33) groundwater with enriched but variable Si concentrations (42–550 μmol L^{-1}) and radium activities (0.6–6 dpm 100 L^{-1} ^{223}Ra; 14–55 dpm 100 L^{-1} ^{224}Ra, and 6–16 dpm 100 L^{-1} ^{226}Ra); mixing diagrams indicate simple two end-member mixing. *Sites*: Kaloko (H3) and Honokohau Beach (H4), Hawai'i; Kamiloloa (MO2), Molokai; Honolua (MA1), Kahana (MA2), Mahinahina (MA3), Maui.
- *Category* 3: High salinity (>34.5), relatively low Si (11–42 μmol L^{-1}) groundwater with moderate enrichment in short-lived Ra (0.9–1.3 dpm 100 L^{-1} ^{223}Ra; 10–15 dpm 100 L^{-1} ^{224}Ra) and ^{226}Ra activities similar to adjacent seawater (~6.5 dpm 100 L^{-1});); mixing diagrams indicate simple two end-member mixing. *Sites*: Puako Bay (H2), Hawai'i and Honokowai (MA4), Maui.

At most Category 1 sites low salinity groundwater input appears to have been accompanied by an additional source of Ra to the coastal zone (defined by our sampling "box"), as indicated by elevated ^{223}Ra and ^{224}Ra activities in nearshore samples. We suspect that this additional Ra source represents saline SGD, consisting largely of seawater circulated through

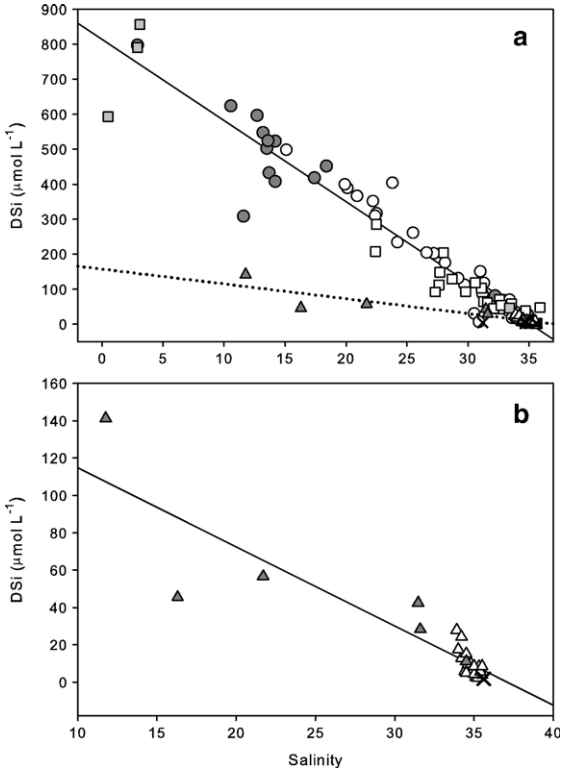

Fig. 5. Correlation between DSi concentration and salinity at (a) all sampling locations and (b) Maui locations only.

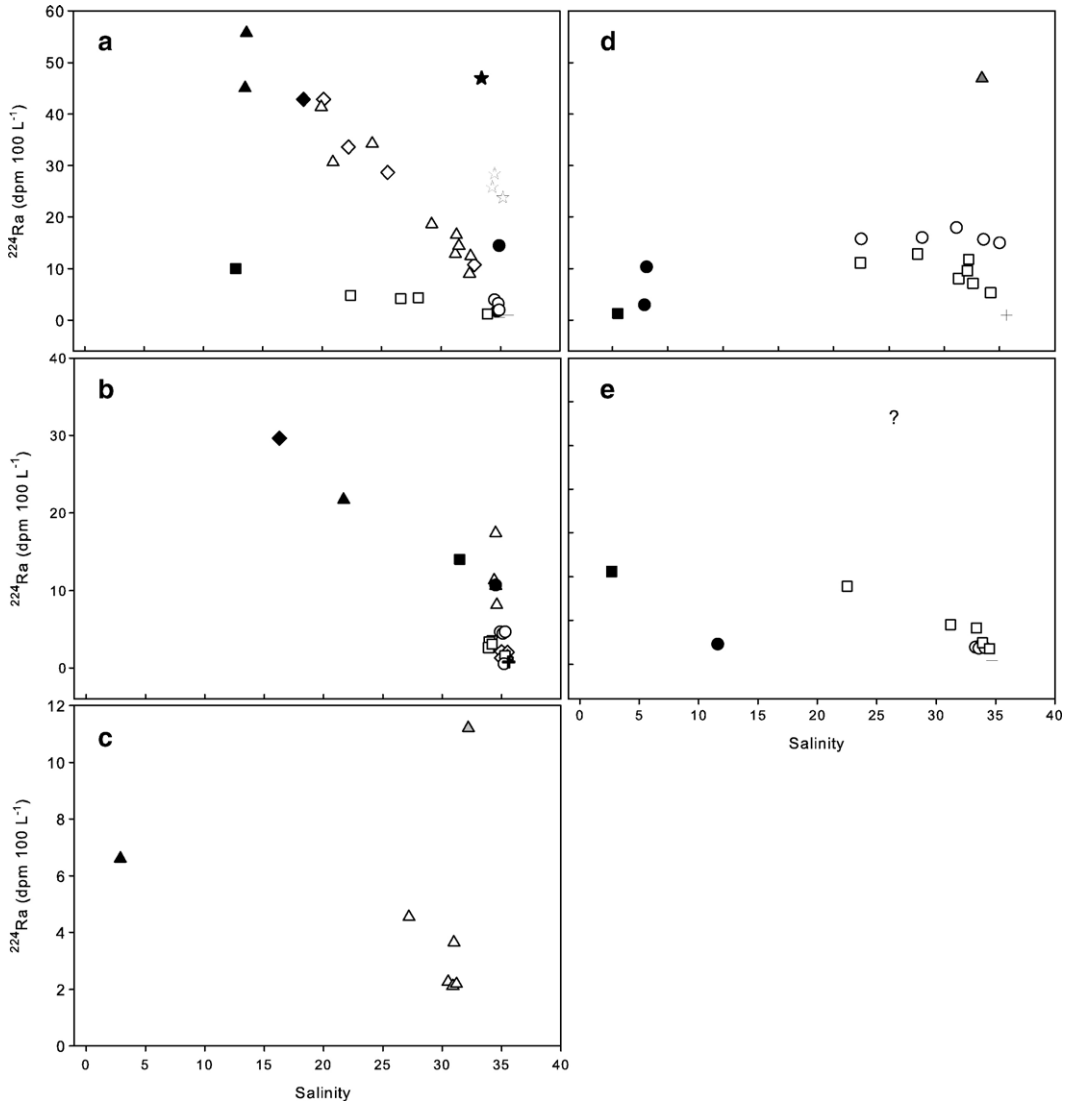

Fig. 6. Nearshore mixing diagrams for all sampling locations using ^{224}Ra and salinity tracers. Groundwater samples are denoted by solid-color shapes; nearshore samples by open shapes. Offshore seawater given as (+). (a) Two end-member mixing between brackish to saline groundwater and offshore seawater at H2 (○), H3 (◇), H4 (△), H7 (□), Hawai'i, and MO2 (★), Moloka'i. (b) Mixing diagram for Maui sites: MA1 (◇), MA2 (△), MA3 (□), MA4 (○). The nearly vertical distribution of nearshore samples suggests two-end-member mixing between saline groundwater and offshore seawater. Brackish groundwater at MA1 and MA2 may make little contribution to nearshore tracer abundances. (c) Nearshore samples at H1 (△) are a mixture of near-fresh groundwater (black), saline groundwater (gray), and offshore seawater end-members. (d) Nearshore samples at MO1 (○) and MO3 (□), Moloka'i, are a mixture of near-fresh groundwater (solid), offshore seawater and an unknown saline end-member (gray △) assumed to be similar to groundwater sampled at MO2. (e) Tracer abundances in nearshore samples at H5 (○) and H6 (□), Hawai'i, appear to be a mixture of near-fresh groundwater (solid), offshore seawater and along with an unknown, saline groundwater end-member or other source of ^{224}Ra.

the shallow unconfined aquifer (Robinson et al., 2007), although diffusion of Ra from bottom sediments may also contribute (Section 3.4.2). At Spencer Beach (H1) a high-Ra, saline groundwater was sampled from a beach well (Fig. 6d); similar high-Ra saline groundwater sources can be inferred from mixing diagrams for Keauhou Bay (H5), Kealekekua Bay (H6), Kapuaiwa Grove (MO1) and Ualapu'e (MO3) (Fig. 6c and e). At the Moloka'i sites, this source may be similar to the saline groundwater sampled at Kamiloloa (MO2). Based on the groundwater samples at H1 and MO2, we estimate that these saline end-members support salinities of 30–35, elevated Ra activities (1 to 2 dpm/100 L ^{223}Ra; 11–47 dpm/100 L ^{224}Ra; 7–10 dpm 100 L^{-1} ^{226}Ra), and intermediate Si concentrations (40–80 μmol L^{-1}) consistent with a seawater-dominated mixture and minor *in situ* accumulation. Honaunau Bay (H7, Fig. 6a) shares the geochemical signature of Category 1, but shows no evidence of additional coastal zone input of Ra.

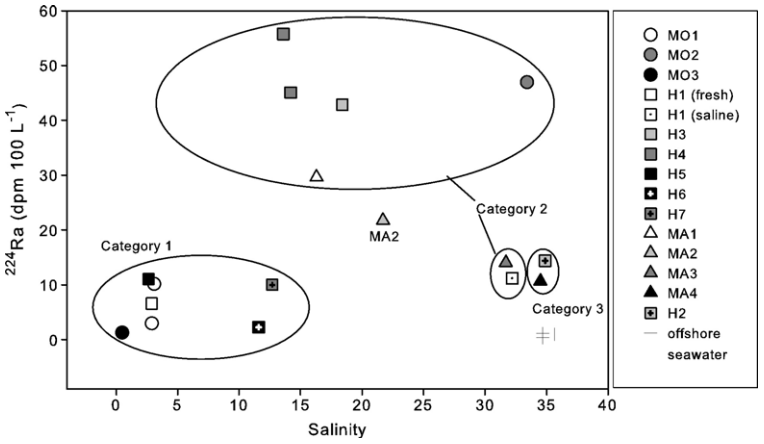

Fig. 7. Categorization of sampling locations based on groundwater salinity and ^{224}Ra activity. MA2 is essentially a subset of Category 2, but with additional Ra input in the coastal zone from an unsampled source (Section 3.1.2). These groupings also hold for the ^{224}Ra and DSi tracers (not shown).

3.2. Modes of groundwater discharge and exchange in the nearshore

On the basis of data presented above we suggest that the high degree of spatial variability in the distribution of tracers among the various sites is linked to differences in the character and timing of groundwater discharge operating at different locations. Li et al. (1999) and Moore (1999) have drawn a distinction between SGD driven by "new", exclusively meteoric groundwater flow and exchange driven by oscillatory processes such as wave set-up and tidal pumping, and it has been argued that these latter processes may account for a large fraction of SGD and chemical transfer in certain places (Valiela et al., 1990a,b; Li et al., 1999; Boehm et al., 2006). All types of SGD are likely to consist of mixtures of fresh groundwater and seawater yet may differ greatly in the relative contributions of these components and the amount of time they spend in contact with rocks and sediments in the coastal aquifer. Low salinity provides an unambiguous signal of meteoric water content in a groundwater sample, and, at least in the Hawai'ian Islands, DSi appears to trace groundwater (generally meteoric) that has experienced prolonged contact with soils, sediment, and rocks.

In contrast, the regeneration rate of radium in an aquifer is determined by the decay constants of the radioactive precursors of the individual Ra isotopes (Moore, 2003). The short-lived isotopes, ^{223}Ra and ^{224}Ra, are regenerated continuously from the decay of their thorium parents (^{227}Th $t_{1/2}$=18.7 d, and ^{228}Th $t_{1/2}$=1.91 yr, respectively), and will thus be somewhat enriched even in groundwater with a short residence time in the coastal aquifer. In contrast to the short-lived isotopes, ^{226}Ra requires considerable time for regeneration from the decay of ^{230}Th ($t_{1/2}=7.5\times10^4$ yr), and will not achieve high activities in an aquifer that is rapidly flushed. Finally, the presence of appreciable amounts of dissolved Ra in any type of groundwater is dependent on salinity; due to particle adsorption, Ra activities are low in groundwater with salinities less than ~10–15. By this reasoning, the activities of ^{223}Ra, ^{224}Ra and ^{226}Ra in groundwater samples, compared to the seawater background, provide a measure of the groundwater residence time in the brackish and saline zones of the coastal aquifer, although it must be noted that other factors (e.g., sediment grain size, redox conditions) can influence the degree of Ra enrichment and that Ra activities may not be uniform in at all levels in the aquifer (Moore 1999; Abraham et al., 2003). Combined with information from the other tracers, the Ra data allow us to describe the mode of SGD, and ultimately the zonation of the subterranean estuary, at each site at the time of sampling. These data can perhaps be best interpreted within the framework of a coastal surficial aquifer consisting of a fresh, meteoric zone, a saline zone, and in between, a mixing zone of variable size and position in relation to the coastline (Fig. 2).

At one extreme, we have Category 1 sites where low salinity, DSi-rich, Ra-depleted water discharged directly from the near-freshwater lens at the shoreline. Strong freshwater discharge presumably pushed the subterranean mixing zone (the zone of Ra-enriched, saline discharge) away from the shoreline, a bit further offshore. Evidence for this saline SGD was found in nearshore samples with short-lived Ra activities in excess of both the near-fresh groundwater and offshore seawater (Fig. 6c–e). While in most cases we do not have direct measurements of this saline groundwater end-member, it is well-established that saline groundwater underlies the freshwater lens in most Hawai'ian surficial aquifers (Lau and Mink 2006). The situation at H1 (Spencer Beach) on Hawai'i differed somewhat in that saline groundwater was sampled from a beach well only ~100 m south of a near-fresh spring discharging from cracks in a basalt bench, demonstrating the importance of structural heterogeneity and focused discharge points, such as springs and lava tubes, in determining the SGD regime at a given site. Nonetheless, both groundwater sources are needed to explain nearshore tracer patterns (Fig. 6c).

At the Category 2 sites (H3, H4, MO2, MA1, MA3), sampled groundwater was characterized by elevated, but variable, Ra activities and DSi concentrations and a range of

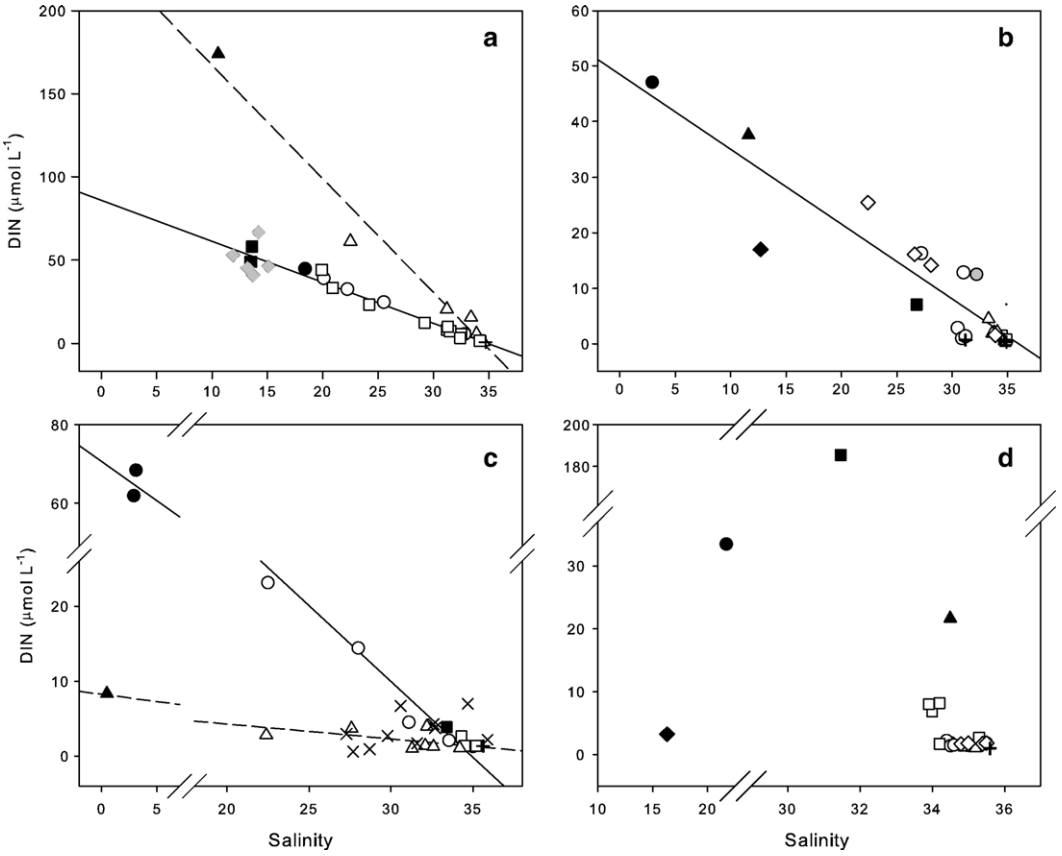

Fig. 8. Relationship between dissolved inorganic nitrogen (DIN) and salinity at all sampling locations. Groundwater samples denoted by solid-color shapes; nearshore samples by open shapes. Offshore seawater given as (+). Breaks in scale are included to clarify patterns at the lower concentrations (a) Central Kona coast locations: H3 (○), H4 (□) and H5 (△). Linear regression lines shown for H3 and H4 samples (solid) and H5 (dashed). (b) Other Hawai'i locations: H1 (○), H2 (□), H6 (△), H7 (◇). Saline groundwater at H1 shown as gray circle. (c) Moloka'i locations: MO1 (○), MO2 (□), MO3 (△) and samples from the alongshore transect (◇). Linear regression lines shown for MO1 (solid) and MO3 (dashed). (d) Maui locations: MA1 (◇), MA2 (○), MA3 (□) and MA4 (△).

brackish salinities reflecting the balance between meteoric groundwater and recirculated seawater at a site at the time of sampling. High activities of short-lived Ra and ^{226}Ra at H3, H4, MA1 and MO2 likely reflect long exchange times in the brackish mixing zone of the coastal aquifer. In Kaloko-Honokohau Park (H3, H4) on Hawai'i in particular the mixing zone of the aquifer appears to be large in extent, as indicated by discharge of brackish water from springs up to a kilometer inland (see Table 2a, "inland spring"). The brackish-saline mixing zone at MA3, in contrast, appears to be more rapidly flushed, as indicated by low enrichments in the short-lived Ra isotopes and ^{226}Ra similar to the seawater background. At each of these sites the subterranean mixing zone appears to intersect with the shoreline.

Kahana (MA2), Maui, presents a special case. On one hand, groundwater sampled at this site contained elevated activities of all three Ra isotopes, moderate DSi concentration, and rather low salinity (21.7), similar to other Category 2 sites; on the other hand, nearshore samples were enriched in short-lived Ra above the two end-member mixing line but were nearly as saline as offshore seawater (Fig. 6b). This combination suggests that in addition to any groundwater end-member that we sampled, another source of Ra exists (either saline SGD or diffusive flux). The situation at this site illustrates both the difficulties of adequately characterizing a complex groundwater system and the utility of using multiple tracers.

The high salinities, low enrichments of short-lived Ra and DSi, and lack of ^{226}Ra enrichment in groundwater at "Category 3" sites (H2, MA4) suggest systems in which aquifer residence times are short, processes such as tidal pumping and wave set-up dominate – potentially operating as shallow, recirculating saline plumes in the upper aquifer (Robinson et al., 2007) – and limited transfer of meteoric groundwater to the coastal ocean occurs. A mixing zone was either absent or went undetected at the time of sampling.

The tracer distributions and implied discharge modes discussed above are likely to vary seasonally, or over the course of a tidal cycle, and a given site may change its

"character" on these timescales. Greater temporal coverage in sampling is needed to understand the dynamics of these systems. However, if nearshore residence times exceed the tidal period (~12 hr), as we have assumed in our conservative calculations, then our nearshore tracer measurements will to a greater or lesser degree provide an integrated picture of SGD at a given site over the full tidal cycle.

3.3. Nutrients in groundwater and nearshore waters

Nutrient concentrations from the various sampling locations are given in Tables 2a, 2b and 2c. Concentrations of inorganic nitrogen and phosphorus in our samples were generally well-correlated with the groundwater tracers (for example, DIN versus salinity shown in Fig. 8a–d). Nonetheless, we observed substantial differences among locations and between the three islands, reflecting the dominant modes of SGD operating at the time of sampling as well as site-specific differences.

3.3.1. Nutrient concentrations in groundwater

In general, the highest nutrient concentrations were detected in groundwater samples containing a substantial meteoric component (categories 1 and 2, above) at most locations on Hawai'i (H1, H3, H4, H5, H6, H7) and Moloka'i (MO1, MO3) (Tables 2a,2b,2c, Fig. 8a–c). Fresh and brackish groundwater collected at these sites contained high concentrations of DSi (588±155 μmol L^{-1}, n=14) soluble reactive phosphate (SRP) (2.61±0.90 μmol L^{-1}) and dissolved inorganic nitrogen (DIN) (55.3±35.8 μmol L^{-1}); on average, nitrate comprised 96% of the nitrogen in these samples. Groundwater DSi concentrations at locations where the meteoric groundwater component was minor (H2, MO2, all Maui sites) were lower (11–57 μmol L^{-1}) but still reflective of groundwater salinity (Fig. 5). N and P concentrations, in contrast, were highly variable (3.26 to 185 μmol L^{-1} DIN, 0.44 to 3.34 μmol L^{-1} SRP) and not always well-correlated with groundwater salinity (Table 2a,2b,2c; DIN shown in Fig. 8b–d. For example, disparate DIN concentrations in saline groundwater samples from Mahinahina (MA3, 185 μmol L^{-1} DIN, S=31.7) and Kamiloloa (MO2, 3.86 μmol L^{-1} DIN, S=33.4) were observed despite their similar salinities. These results emphasize the importance of local factors, such as the degree of anthropogenic influence, in determining the nutrient loads being delivered to the coastal zone via SGD.

Nutrient concentrations detected by Kay et al. (1977) and Dollar and Atkinson (1992) in fresh and brackish groundwater (29–95 μmol L^{-1} NO_3^-, 1–4 μmol L^{-1} PO_4^{3-}; 770–974 μmol L^{-1} Si) at several Kona-Kohala coast locations were consistent with those measured in our typically more brackish, seawater-diluted groundwater samples on this island. High P and Si concentrations are expected in pristine groundwater on Hawai'i due to the rapid weathering of the young basalts (10^3–10^5 yrs) that make up the leeward coast (Crews et al., 1995; Vitousek et al., 1997; Lau and Mink, 2006). In contrast, we might expect the greater degree of weathering and leaching of mobile P from the older, more developed soils on Maui and Moloka'i to result in lower groundwater SRP concentrations relative to Hawai'i (Crews et al., 1995, Vitousek et al., 1997). In fact, no such clear pattern was observed, with near-fresh groundwater SRP concentrations on Moloka'i being similar to those on Hawai'i.

High N concentrations in groundwater may be related to large pools of total N and high rates of remineralization in thin upland soils, particularly on the Big Island (Crews et al., 1995), and to high rates of N-fixation associated with plants, such as the *kiawe* tree, common to leeward coastal areas (Kay et al., 1977; Lau and Mink 2006). In certain locations, however, it is likely that human activities are contributing N and P to the groundwater. For instance, it has been shown previously that fertilizer leaching from golf courses may double the N load of SGD at Keauhou Bay (H5) (Dollar and Atkinson 1992), a site at which we detected extremely high concentrations of DIN (174 μmol L^{-1}). Similarly, leaching from golf courses and pineapple fields has been linked to high nitrate concentrations in West Maui groundwater (Soicher and Peterson 1997), and may explain the high concentrations of DIN in the rather saline groundwater at Mahinhina (MA3).

3.3.2. Nutrient concentrations in the coastal zone

To a large extent, nutrient concentrations in the coastal zone at our sampling sites reflected the degree of N, P and Si enrichment detected in groundwater sources (DIN shown in Fig. 8). However, the nearshore distributions of nutrient compounds may also be influenced by biological cycling and other non-conservative processes. Average nearshore nutrient concentrations on Hawai'i (0.83±0.72 μmol L^{-1} SRP; 13.6±14.9 μmol L^{-1} DIN; 114±125 μmol L^{-1} DSi: n=34) were typically 2 to 20 times greater than concentrations in offshore seawater (0.18±0.01 μmol L^{-1} SRP, 0.66±0.24 μmol L^{-1} DIN, 6.0±6.4 μmol L^{-1} DSi μmol L^{-1} DSi, n=4). N inventory, as with the groundwater samples, was dominated by nitrate (95%). Coefficients of determination (COD) for samples from all sites but Keauhou Bay (H5) demonstrate that DSi, salinity, and ^{224}Ra can account for 97%, 92% and 75%, respectively, of the variance (p<0.001) in nearshore DIN concentrations, and 94%, 90%, and 65% of the variance (p<0.001) in nearshore SRP concentrations. Similarly strong relationships are observed for DIN at Keauhou Bay (Fig. 8a) but with different slopes due to the high concentrations of nitrate measured at this site. Fig. 8a and b depict the close relationship between salinity and DIN in nearshore samples. These results indicate that SGD is the major source of N and P to the coastal zone of leeward Hawai'i, and that mixing, rather than biological uptake or cycling, determined their distribution at the time of sampling.

Nearshore nutrient concentrations off Moloka'i (0.78±0.46 μmol L^{-1} SRP; 3.86±4.75 DIN μmol L^{-1}, 99.9±127 μmol L^{-1} DSi, n=27) were more variable, with DIN concentrations noticeably lower than on Hawai'i, though still in excess of offshore values (0.72 μmol L^{-1} SRP, 1.36 μmol L^{-1} DIN, 1.48 μmol L^{-1} DSi). The relatively low DIN concentrations, low N:P ratios, and large ammonium fraction of DIN (~35%) in nearshore samples likely reflect active N uptake and cycling in the extensive south Molokai back-reef area. Fig. 8c shows the

relationship between DIN and salinity in all nearshore samples. COD for all nearshore indicate that salinity can account for 28%, 40% and 66% of the variance ($p<0.01$) in nearshore DIN, nitrate and SRP concentrations, respectively (similar results are obtained for DSi as the independent variable). The weaker correlations (in comparison to Hawai'i) result in part from different DIN-salinity trends at MO1 and MO3, but likely also reflect a greater degree of nearshore N and P cycling. Nonetheless, it is clear that SGD is an important source of nutrients along this coast. Radium activities and nutrient concentrations at most of these sites were only weakly correlated, as was expected given the widespread discharge of fresh, Ra-depleted but nutrient-rich groundwater along the Molokai shore, as indicated in Fig. 6c.

Nearshore DIN concentrations off West Maui were uniformly low (1.67 ± 0.34 μmol L^{-1}, $n=10$), scarcely above the offshore value (~1 μmol L^{-1}), with the exception of Mahinahina (MA3; 6.21 ± 3.04 μmol L^{-1}, $n=4$). Nearshore SRP concentrations were also relatively low (0.42 ± 0.27 μmol L^{-1}, $n=14$) but more in line with the other islands. Nearshore DSi concentrations (10.8 ± 0.34 μmol L^{-1}) were enriched above offshore water (1.84 μmol L^{-1}) but much lower than at the other islands. Weak correlations among nearshore Ra activities, DSi, salinity and DIN and SRP concentrations at these sites (Fig. 8d — DIN versus salinity) indicate that processes other than simple dilution (e.g., biological uptake and cycling on land and in the coastal zone) determine the spatial distributions of these non-conservative nutrients, but does not rule out a groundwater source.

3.4. Box model calculations of groundwater discharge and associated nutrients

Groundwater discharge and its contribution to the nutrient budget of adjacent marine waters was estimated at each site using Eqs. (1), (2), (3), (4a), (4b) and applying water exchange times (τ) based on available current measurements (Presto et al., 2006; Storlazzi et al., 2006) and/or nearshore $^{224}Ra/^{223}Ra$ activity ratios (Eq. (5)), representing lower and upper estimates of τ. The actual residence time of water in the coastal zone may vary greatly among sites due to irregularities in the coastline and nearshore bathymetry, and over time at a single site due to changing current and wave conditions. Calculated rates of SGD should thus be considered first order approximations. In light of the highly uncertain nature of the current-derived residence times in particular, our discussion and conclusions are based on the more conservative discharge estimates. Results and input parameters are presented in Tables 3a, 3b and 4.

3.4.1. Submarine groundwater discharge

SGD fluxes calculated based on the two end-member mass balance (Eqs. (2) and (3); Tables 3a and 3b) ranged from 0.02–0.65 $m^3\ m^{-2}\ d^{-1}$, using the more conservative estimates of τ at each site. At sites where current velocity measurements were available, SGD fluxes based on minimum nearshore exchange time estimates were 1–2 orders of magnitude greater, ranging from −4.1–18.5 $m^3\ m^{-2}\ d^{-1}$. At sites where two types of SGD were identified – H1 (Spencer Beach), MO1 (Kapuaiwa Grove) and MO3 (Ualapu'e) – the three end-member mixing model described in Eqs. (4a) and (4b) yielded separate flux estimates for saline and near-fresh groundwaters, in addition to a total SGD flux (Table 4). Total SGD flux at these sites ranged from 0.12–0.39 $m^3\ m^{-2}\ d^{-1}$ (conservative τ), with 49–77% occurring as saline discharge. Flux estimates based on current velocities at the Molokai sites were 1–2 orders of magnitude greater (5.1–15.7 $m^3\ m^{-2}\ d^{-1}$). The 20- to 30-fold range in our estimates of SGD at these sites is yet another indicator of the high degree of spatial heterogeneity in the coastal groundwater regime on these islands. Calculated SGD fluxes were greatest at Honokohau Beach (H4) on Hawai'i, at low tide.

The various tracers measured (^{224}Ra, ^{223}Ra, salinity, and Si) were used to generate a range of SGD flux estimates at each site (Tables 3a,3b, 4). These estimates are in general agreement with one another, supporting our contention that the chosen tracers share a common source (SGD) and are largely conservative in the nearshore zone. ^{226}Ra-based discharge estimates are in most cases much lower than the others due to the small degree of ^{226}Ra enrichment in groundwater samples relative to offshore seawater (~6.0–6.5 dpm 100 L^{-1}). Because the regeneration time of ^{226}Ra from its long-lived precursors is long, it will not be greatly enriched in a rapidly flushed coastal aquifer. It is also notable that the short-lived Ra tracers yielded the highest flux estimate at six of the nine sites evaluated using the two end-member model; this likely reflects the additional source(s) of ^{224}Ra and ^{223}Ra implied in our observations — that is, SGD input or diffusive flux of Ra from sediments within the coastal zone, away from the shoreline (see Fig. 3).

The SGD rates calculated in this study fall within the range of previously published estimates for the Hawai'ian Islands and provide an interesting comparison to disparate sites from other parts of the world (Table 5). Previous estimates of fresh SGD for Kona coast locations (Keauhou Bay, Waikoloa, Kaloko-Honokohau NP) (Kay et al., 1977; Dollar and Atkinson 1992; Oki et al., 1999) range from 0.12–0.30 $m^3\ m^{-2}\ d^{-1}$, similar to our conservative flux estimates ($\tau=1.5$ d) for this coast, though our estimates include both fresh and saline discharge. The high fluxes reported by Paytan et al. (2006) for Puako Bay far exceed our conservative estimates for the same location, but were based on a shorter estimate of the nearshore residence time and were collected at a different location on the bay. Garrison et al. (2003) reported a total SGD input of 90,000 $m^3\ d^{-1}$ to Kahana Bay, on windward Oahu, which if distributed over the study area of approximately 1.6 km^2 would translate into an areal flux of 0.06 $m^3\ m^{-2}\ d^{-1}$, comparable to many of our sites.

The range of SGD estimates for sites dominated by saline groundwater (H2, MO2, all Maui sites), 0.02–0.33 $m^3\ m^{-2}\ d^{-1}$, overlapped with SGD estimates from other semi-arid to arid coastlines where recirculation of seawater (via tidal pumping and wave set-up) is thought to be the main driver of fluid exchange between the unconfined aquifer and coastal ocean. Boehm et al. (2004) and Shellenbarger et al. (2006) calculated SGD fluxes of 0.06–0.9 $m^3\ m^{-2}\ d^{-1}$ and 0.06–0.26 $m^3\ m^{-2}\ d^{-1}$ for Huntington Beach, California and the northern Gulf of Aqaba, respectively. Our results further support the idea that recirculation processes can lead to large SGD fluxes and can represent an important route of chemical

Table 3a
Discharge of groundwater, dissolved inorganic N (TIN, $NO_3^- + NO_2 + NH_4^+$), soluble reactive phosphate (SRP) and silica (SiO_4) to the nearshore on Hawai'i

Site #	Location	Tide	Box vol. (m^3)	τ	GW type	SGD — by tracer ($m^3\ d^{-1}$)					SGD flux ($m^3\ m^{-2}\ d^{-1}$)	N and P fluxes (mmol $m^{-2}\ d^{-1}$) (range of estimates)	
						^{224}Ra	^{223}Ra	^{226}Ra	DSi	Sal.		DIN	SRP
H2	Puako Bay	High	25	1.56 d	Saline	2.8	2.0	–	3.5	–	0.04–0.07	0.28–0.50	0.04–0.07
H3	Kaloko	Low	1200	1.56 d	Brackish	642	512	(244)	437	446	0.31–0.46	14.0–20.5	0.84–1.2
	Fishpond			0.7 hr		25,902	24,347	(8116)	22,739	23,201	16.3–18.5	727–828	44–50
H4	Honokohau	High-ebb	1375	1.56 d	Brackish	321	189	(132)	136	144	0.1–0.23	4.8–11.5	0.24–0.57
	Beach	Low	1375	1.56 d	Brackish	896	535	(192)	598	564	0.39–0.65	19.1–32.0	0.96–1.6
		Flood-high	1375	1.56 d	Brackish	279	159	(165)	158	156	0.11–0.20	6.6–11.8	0.30–0.54
H5	Keauhou Bay		15,000	1.56 d	Brackish	–	–	–	2407	1771	0.17–0.23	29–40	0.68–0.93
H6	Kealekekua Bay	Flood	53.3	1.56 d	Brackish	–	–	–	2.7	0.8	0.03–0.11	1.2–4.0	0.03–0.10
H7	Honaunau Bay	Ebb	650	1.56 d	Brackish	218	173	–	191	167	0.19–0.25	3.7–4.3	0.55–0.63

Based on measurements of ^{223}Ra, ^{224}Ra, ^{226}Ra, [DSi], and salinity; two end-member model.

transfer between the unconfined aquifer and coastal ocean (Li et al., 1999; Boehm et al., 2004; Shellenbarger et al., 2006).

At sites with a substantial meteoric component SGD fluxes of 0.03–0.65 $m^3\ m^{-2}\ d^{-1}$ ($\tau = 1.5$ d) were estimated (see Tables 3a,3b, 4), overlapping or exceeding flux estimates for much wetter coastlines (Table 5). The large magnitude and wide range of SGD estimates in this study likely reflect the unique features of leeward Hawai'i: Semi-arid coastlines in close proximity to high-rainfall uplands; high groundwater recharge rates; steep topography. Moreover, the volcanic origin of the islands allows for rapid transport through permeable, fractured lava flows, resulting in heterogeneous coastal discharge and high rates of SGD at focused discharge points (Oki et al., 1999). Similarly high SGD fluxes have been reported for the volcanic island of Jeju, South Korea (~0.44 $m^3\ m^{-2}\ d^{-1}$; Table 5) (Hwang et al., 2005).

3.4.2. Diffusive fluxes of tracers from sediments

The declining offshore gradients in Ra activities and DSi concentrations and high values in groundwater samples suggest a dominant SGD source of these tracers. However, another potential source that we did not explicitly consider in our mass balance is diffusive flux from bottom sediments (Rama and Moore 1996; Shellenbarger et al., 2006). Nearshore sediments on these islands consist of coarse, weathered basaltic sands and gravels with variable amounts of coral fragments. The low abundances of Ra precursors in these mafic source materials (Gascoyne 1992) are reflected in the relatively low groundwater Ra activities observed in this study, and will limit the sedimentary supply of Ra. Moreover, in the high-energy nearshore zone, we expect that the advection of fluid in and out of pore spaces in the coarse sediments will account for much of the transfer of dissolved Ra from the sediments to the water column (Precht and Huettel 2003) and will supply some of the excess Ra we measure in the control box. Diffusive fluxes of ^{226}Ra from bottom sediments are expected to be negligible due to the slow production rate of ^{226}Ra from ^{230}Th (Rama and Moore 1996), but measurable diffusive fluxes of ^{223}Ra and ^{224}Ra are likely to occur (Rama and Moore 1996; Charette et al., 2001; Hwang et al., 2005). Diffusive fluxes of DSi generated in bottom sediments from remineralization of siliceous organic matter or weathering of basalt grains may also contribute to the nearshore budget of this tracer (Hwang et al., 2005). It is likely that neglecting diffusion from sediments has led us to overestimate total and saline SGD fluxes based on Ra and DSi mass balances, as may be reflected in the higher Ra-based SGD rates (Tables 3a,3b and 4)

Table 3b
Discharge of groundwater, dissolved inorganic N (TIN, $NO_3^- + NO_2 + NH_4^+$), soluble reactive phosphate (SRP) to the nearshore on Maui and Moloka'i

Site #	Location	Tide	Box vol. (m^3)	τ	GW type	SGD — by tracer ($m^3\ d^{-1}$)					SGD flux ($m^3\ m^{-2}\ d^{-1}$)	N and P fluxes (mmol $m^{-2}\ d^{-1}$) (range of estimates)	
						^{224}Ra	^{223}Ra	^{226}Ra	DSi	Sal.	Range	DIN	SRP
MA1	Honolua Bay	High-ebb	7900	3 d	Brack-saline	1043	140	–	328	91	0.02–0.17	0.05–0.58	0.01–0.07
MA2	Kahana	High	27.7	1.56 d	Brack-saline	10.7	10.3	(1.3)	4.4	4.9	0.07–0.18	2.4–6.0	0.06–0.15
				0.6 hr		467	530	(75)	245	274	4.1–8.8	137–300	3.3–7.2
MA3	Mahinahina	Low	42	1.56 d	Brack-saline	3.9	5.5	–	3.6	9.9	0.07–0.20	13.3–36.8	0.06–0.15
MA4	Honokowai	Flood	22.5	1.56 d	Saline	7.1	4.7	–	2.5	–	0.06–0.16	1.2–3.4	0.01–0.02
MO2	Kamiloloa	Ebb	5925	1.56 d	Brack.-saline	2619	2188	(480)	1429	1641	0.18–0.33	0.70–1.3	0.16–0.30
				0.8 hr		91,453	89,978	(16,749)	64,192	73,714	8.1–11.6	31.5–44.9	7.2–10.3

Based on measurements of ^{223}Ra, ^{224}Ra, ^{226}Ra, [Si], and salinity; two end-member model.

Table 4
Discharge of groundwater, dissolved inorganic N (DIN, $NO_3^- + NO_2 + NH_4^+$), soluble reactive phosphate (SRP) to the nearshore at Spencer Beach, Hawai'i (H1) and Kapuaiwa Grove (MO1) and Ualapu'e (MO3), Molokai

Site #	Location	Tide	Box vol. (m^3)	τ	GW type	SGD (m^3 d^{-1}) — by tracer combo				SGD flux (m^3 m^{-2} d^{-1})	N and P fluxes (mmol m^{-2} d^{-1}) (range of estimates)	
						^{224}Ra+DSi	^{224}Ra+Sal	^{223}Ra+DSi	^{223}Ra+Sal		DIN	SRP
H1	Spencer Beach	Low	9750	2.6 d	Fresh	354	507	384	526	0.05–0.07	2.2–3.2	0.06–0.08
					Saline	844	754	546	512	0.07–0.11	0.84–1.4	0.05–0.08
					Total	1199	1261	930	1037	0.12–0.17	3.3–4.4	0.11–0.15
MO1	Kapuaiwa Grove	Low-flood	60	1.56 d	Fresh	5.6	5.7	5.5	5.6	0.09–0.095	5.7–5.9	0.18–0.19
					Saline	16.4	16.4	17.9	17.8	0.27–0.30	1.1–1.2	0.24–0.26
					Total	22.0	22.1	23.4	23.4	0.37–0.39	6.8–7.0	0.43
				0.8 hr	Fresh	248	255	239	245	4.0–4.3	246–263	8.0–8.6
					Saline	547	546	700	699	9.1–11.7	35.3–45.3	8.1–10.4
					Total	795	801	939	944	13.25–15.7	291–299	16.4–18.6
MO3	Ualapu'e	Flood	5490	1.56 d	Fresh	406	496	405	495	0.05–0.06	0.38–0.46	0.18–0.22
					Saline	843	840	848	845	0.09	0.36–0.37	0.08
					Total	1249	1336	1253	1340	0.14–0.15	0.74–0.82	0.27–0.31
				0.8 hr	Fresh	18010	21733	17609	21415	2.0–2.4	16.3–20.2	7.9–9.7
					Saline	28199	28095	33321	33168	3.1–3.7	12.1–14.4	2.8–3.3
					Total	252	273	278	298	5.1–6.1	28.9–34.2	10.9–12.9

Based on measurements of ^{223}Ra, ^{224}Ra, ^{226}Ra, [DSi], and salinity, and a three end-member model.

at several sites. Even in the most extreme case, however, Ra-based SGD estimates are of the same order as estimates based on DSi and salinity. The general consistency among tracers suggests that diffusive fluxes do not affect our basic conclusions about SGD along these coasts. Future work will quantify the importance of sedimentary diffusion in tracer budgets.

3.4.3. Tidal variability

As displayed in Table 2a, nearshore ^{223}Ra and ^{224}Ra activities and DSi concentrations at Honokohau Beach (H4) were 2–3 times greater, and salinity significantly lower, at low tide than at high tide, resulting in a commensurate increase in the estimated input of SGD and nutrients to the coastal zone (Table 3a). The low to high tide activity differential was much smaller for ^{226}Ra, as expected from the lower enrichment of this isotope in the groundwater end-member and its long regeneration time.

It is notable that the sites we have classified as being dominated by recirculated seawater (Puako Bay (H2), Hawai'i; Honokowai (MA4), Maui) were sampled at high or flood tides. As a result, we may have failed to capture low/ebb tide discharge of freshened groundwater at these sites, although as discussed above, we expect that our tracers time-integrate SGD to some extent. We almost certainly underestimated SGD at other sites that were sampled at high tide (e.g., MA2, MO3). However, we found no clear relationship between tidal height and tracer abundances or SGD fluxes among the various sites. While tides are an important modulator of SGD in Hawai'i, as elsewhere, it is difficult to attribute the major differences between sites to the timing of sampling in the tidal cycle.

3.4.4. Groundwater nutrient additions

Our estimates of the groundwater contributions of DIN and SRP to the nearshore are presented in Tables 3a,3b, and 4. DIN additions from SGD ranged widely, from 0.05 to 40 mmol N m^{-2} d^{-1}, or 0.25 to 205 g N m^{-2} yr^{-1}. The highest rates of nitrogen input (>6 mmol N m^{-2} d^{-1}) occurred at Keauhou Bay (H5), Kaloko (H3), and Honokohau Beach (H4) on Hawai'i, Mahinahina (MA3) on Maui, and Kapuaiwa Grove (MO1) on Molokai. Each of these sites was characterized by relatively high discharge of low salinity groundwater and/or high DIN concentrations. SRP additions from SGD ranged from 0.01 to 1.6 mmol P m^{-2} d^{-1} (0.1 to 18 g P m^{-2} yr^{-1}). High rates of SRP input (>0.25 mmol P m^{-2} d^{-1}) occurred at the Hawai'i sites mentioned above (H3, H4, H5), as well as at Honaunau Bay (H7) and all three Molokai locations, reflecting the high P concentrations measured in groundwater at these sites. As a general matter, nutrient additions – especially DIN – were greater at sites displaying active discharge of lower salinity groundwater with a large meteoric component. However, it is clear that large nutrient loads can also be delivered via predominantly saline SGD, due in part to high volumes of exchange even when nutrient concentrations are moderate. For instance, at the three locations (H1, MO1, MO3) where separate near-fresh and saline-groundwater nutrient fluxes were estimated, the saline component accounted for 18–48% of the total nutrient load (Table 4). Predominantly saline discharge at three Maui locations (MA2, MA3, MA4) delivered nutrients at a rate comparable to or greater than those found at other sites discharging fresher water. The saline component of SGD should not be neglected, particularly at sites suspected to be affected by pollution (e.g., Mahinahina, Honokowai, Maui).

Our calculations of SGD nutrient additions neglect the probability that some fraction of the nutrients detected in our typically brackish to saline groundwater samples entered the aquifer with recirculated seawater, and thus cannot be considered "new" nutrients. An exact accounting of new versus recycled nutrients in the unconfined aquifer-coastal zone system

Table 5
A comparison of DIN and SRP fluxes via SGD at various coastal sites

Location	SGD flux m^3 m^{-2} d^{-1}	DIN flux mmol N m^{-2} d^{-1}		DIP or SRP fluxes mmol P m^{-2} d^{-}	Reference
Hawai'ian Islands					
Keauhou Bay, Hawaii	0.30 [a]	22.5		1.2	Kay et al., 1977, Dollar and Atkinson 1992
Waikoloa, Hawaii	0.21 [a]	17.3		0.33	Kay et al., 1977, Dollar and Atkinson 1992
Kaloko-Honokohau, Hawaii	0.12 [a]	–		–	Oki et al., 1999
Puako Bay, Hawaii	2.0–2.6	330		–	Paytan et al., 2006
Kahana Bay, Oahu	0.11 [b]	3.4 (TDN)		0.17 (TDP)	Garrison et al., 2003
Other sites					
Eilat, Israel	0.06–0.26	2.9–10		0.02–2.0	Shellenbarger et al., 2006
Huntington Beach, California	0.06–0.92 [a]	0.7–12		0.04–0.54	Boehm et al., 2004
Jeju, South Korea	0.44	21.4		0.16	Hwang et al., 2005
North Inlet, S. Carolina	0.03	2.42		0.91	Krest et al., 2000
Gulf of Mexico, Florida	0.1–0.11	–		–	Corbett et al., 1999, Moore 2003
Pettaquamscutt, Rhode Is.	0.002–0.02	0.17–0.49		0.01–0.04	Kelly and Moran 2002
Present study — selected sites			% new N		
H1 — Spencer Beach	0.12–0.17	3.3–4.4	89	0.11–0.15	Present study
H2 — Puako Bay	0.04–0.07	0.28–0.50	95	0.04–0.07	
H3 — Kaloko	0.31–0.46	14–21	98	0.84–1.2	
H4 — Honokohau, low tide	0.39–0.65	19–32	99	0.96–1.6	
H5 — Keauhou Bay	0.17–0.23	29–40	99	0.68–0.93	
MO1 — Kapuaiwa Grove	0.37–0.39	6.8–7.0	94	0.42–0.45	
MO2 — Kamiloloa	0.18–0.33	0.7–1.3	74	0.16–0.30	
MA3 — Mahinahina	0.07–0.20	13–37	99	0.06–0.18	

The percentages of "new" nitrogen for sites in the present study are calculated as the excess DIN concentration in groundwater samples after the seawater background is subtracted.

[a] Total discharge (m^3 m^{-1} d^{-1}) from the original studies assumed to be distributed over an area extending offshore to: (a) 75 m at Keauhou and (b) 60 m at Waikoloa and Kaloko-Honokohau NP, as in the present study; (c) 25 m at Huntington Beach, equal to the cross-shore box dimension used in this study (Boehm et al., 2004).

[b] Total discharge to Kahana Bay (~90,000 m^3 d^{-1}) assumed to be distributed over the entire study area (~0.8 km^2).

requires more detailed knowledge of the mechanisms and timescales of exchange than is currently available for these sites. Nonetheless, the typically large difference in nutrient concentration between groundwater and offshore seawater at our sites is one indication that most of the SGD nutrients are new to the system (Table 5). By this simple measure, the groundwater nutrient "excess" (above background seawater) ranges from 65 to >99% of the total DIN, and from 19 to 96% of the total SRP, with most samples in the upper ends of these ranges.

The range of SGD nutrient additions to the nearshore calculated in this study is high relative to published studies from other parts of the world, including sites with similar or greater SGD fluxes, but is of the same order as estimates from other published studies in the Hawai'ian Islands (Table 5). DIN fluxes in particular tend to be high; SGD N fluxes at certain sites (e.g., H3, H4, H5, MO1, MA3) are ~1–2 orders of magnitude greater than those estimated for sites in the eastern United States (e.g., Krest et al., 2000; Kelly and Moran 2002). Groundwater nutrient concentrations at a number of our sites (H1, H5, H6, MO1, MA2, MA3, MA4) are characterized by high N:P ratios (30–55) relative to the Redfield ratio (16). High N:P ratios at Mahinahina (MA3) and Honokowai (MA4) may indicate anthropogenic contamination (e.g., sewage or fertilizer application) at these heavily developed sites.

The high groundwater nutrient fluxes detected at many sites are particularly significant in comparison to the uniformly low-nutrient concentrations present in offshore waters. In the absence of surface runoff, SGD appears to be the dominant source of new nutrients to fringing coral reef and other coastal ecosystems on the leeward shores of these islands. For comparison, our estimates of N input from SGD are 2 to 100 times greater than N-fixation in coral reefs, which has been estimated to be about 0.1 g N m^{-2} yr^{-1} (Dubinsky, 1990). Soicher and Peterson (1997) have suggested that ephemeral streamflow on West Maui can deliver concentrated pulses of freshwater and nutrients to the coast following rainstorms, but that groundwater discharge probably represents the larger, more continuous and evenly distributed source of nutrients. Our data do not contradict this idea; in all cases, our sampling took place at times or locations where streamflow was absent or inactive. Under such conditions, the importance of nutrient additions delivered by groundwater may be magnified.

Assuming a C:N ratio typical of coral reefs (~20) (Atkinson and Smith, 1983), the SGD-derived new DIN fluxes for a selection of our sites (Table 5) could, in theory, support 0.06–9.6 gC m^{-2} d^{-1} of new production. On a reef flat of typical productivity (~8 gC m^{-2} d^{-1}) (Atkinson and Falter 2003), this DIN flux from SGD could support 1–120% of primary production. A more conservative calculation based only on fresh SGD N additions at

the sites H1, MO1, and MO3 yields new production rates of 0.09–1.4 gC m^{-2} d^{-1}, or 1–18% of "typical" primary production. The relevance of such simple, ratio-based calculations is equivocal, however, and potentially site-specific. Nutrient uptake by reef communities of coral and algae is thought to be mass transfer limited (Steven and Atkinson 2003), and thus the fraction of nutrient removed from water flowing past reef benthos may be small. This is particularly true of sites with strong horizontal mixing and/or vertical stratification of the water column, which may limit contact between fresh, nutrient-rich runoff or SGD and the reef (Atkinson and Falter 2003; Dollar and Atkinson 1992). Sites with longer water residence times, such as several of the semi-enclosed bays in this study (e.g., MA1, H1), as well as the broad, shallow Molokai back-reef, may be more vulnerable to adverse effects from SGD nutrient additions than the more high-energy sites. Further work is needed to better understand the dynamics and possible ecosystem effects of SGD nutrient additions, which we have demonstrated to be large and widespread along the leeward coasts of Hawai'i, Maui, and Moloka'i.

4. Conclusions

Several important conclusions can be drawn from this work. First, a multiple-tracer approach offers distinct advantages for characterizing SGD along leeward Hawai'i due to the diverse (and potentially variable) array of discharge modes occurring between sites. Low salinities and high DSi concentrations provide an unambiguous signal of meteoric groundwater input, while Ra isotopes capture discharge in the brackish to saline range, including seawater recirculation that can be difficult or impossible to characterize using salinity alone. Moreover, measurements of both short- and long-lived Ra isotopes provide one means of gauging the timescales of exchange between the coastal aquifer and nearshore zone, and between nearshore and offshore waters. Although SGD nutrient loads were highly variable among the sites, meteoric groundwater is nonetheless a major (and in some cases, the dominant) source of new nutrients to coastal ecosystems in leeward Hawai'i, Maui, and Moloka'i. At particular sites, (e.g., Mahinahina, Maui) saline SGD and seawater exchange with the unconfined aquifer represent an important pathway for nutrient transfer to the nearshore zone, and should not be overlooked in coastal nutrient budgets. Nutrient and other pollutant loads associated with SGD warrant further study, particularly in locations where coastal development and management of coastal resources are growing concerns.

Acknowledgments

We thank Ali Boehm, Katy Elsbury, Scott Wankel, Ashley Ivy, Megan Young, Gaurav Misra and the USGS Coral Reef research group for assistance with sample collection and Ra analyses. Thanks are also due to the staff of Kaloko-Honokohau National Historic Park for facilitating access to sampling sites. Billy Moore, Ali Boehm, Matt Charette and two anonymous reviewers provided useful advice and comments during the preparation of the manuscript. This research was funded in part by grants to AP from the Stanford UPS Urbanization Research Fund, the Meade Foundation and the National Park Service.

References

Abraham, D.M., Charette, M.A., Allen, M.C., Rago, A., Kroeger, K.D., 2003. Radiochemical estimates of submarine groundwater discharge to Waquoit Bay, Massachusetts. Biol. Bull. 205, 246–247.

Atkinson, M.J., Falter, J.L., 2003. Coral reefs. In: Black, K.D., Shimmield, G.B. (Eds.), Biogeochemistry of Marine Systems. CRC Press, Boca Raton, FL, pp. 40–64.

Atkinson, M.J., Smith, S.V., 1983. C:N:P ratios of benthic marine plants. Limnol. Oceanogr. 28, 568–574.

Boehm, A.B., Paytan, A., Shellenbarger, G.G., Davis, K.A., 2006. Composition and flux of groundwater from a California beach aquiver: implications for nutrient supply to the surf zone. Cont. Shelf Res. 26, 269–282.

Boehm, A.B., Shellenbarger, G.G., Paytan, A., 2004. Groundwater discharge: a potential association with fecal indicator bacteria in the surf zone. Environ. Sci. Tech. 38, 3558–3566.

Cesar, H.S.J., Van Beukering, P.J.H., 2004. Economic valuation of the coral reefs of Hawai'i. Pac. Sci. 58 (2), 231–242.

Charette, M.A., Buesseler, K.O., Andrews, J.E., 2001. Utility of radium isotopes for evaluating the input and transport of groundwater-derived nitrogen to a Cape Cod estuary. Limnol. Oceanogr. 46, 465–470.

Corbett, D.R., Chanton, J., Burnett, W., Dillon, K., Rutkowski, C., Fourqurean, J.W., 1999. Patterns of groundwater discharge into Florida Bay. Limnol. Oceanogr. 44, 1045–1055.

Crews, T.E., Kitayama, K., Fownes, J.H., Riley, R.H., Herbert, D.A., Mueller-Dombois, D., Vitousek, P.M., 1995. Changes in soil phosphorus fractions and ecosystem dynamics across a long chronosequence in Hawaii. Ecology 76 (5), 1407–1424.

D'Elia, C.F., Webb, K.L., Porter, J.W., 1981. Nitrate-rich groundwater inputs to Discovery Bay, Jamaica: a significant source of N to local coral reefs? Bull. Mar. Sci. 31, 903–910.

Dollar, S.J., Atkinson, M.J., 1992. Effects of nutrient subsidies from groundwater to near shore marine ecosystems off the island of Hawaii. Estuarine, Coast. and Shelf Sci. 35, 409–424.

Dubinsky, Z., 1990. Ecosystems of the World 25: coral reefs. Elsevier, New York.

Garrison, G.H., Glenn, C.G., McMurtry, G.M., 2003. Measurement of submarine groundwater discharge in Kahana Bay, Oahu, Hawai'i. Limnol. Oceanogr. 48, 920–928.

Gascoyne, M., 1992. Geochemistry of the actinides and their daughters. In: Ivanovich, M., Harmon, R.S. (Eds.), Uranium-series Disequilibrium: Applications to Earth, Marine, and Environmental Sciences. Clarendon Press, Oxford, UK, pp. 34–61.

Hatcher, B.G., 1997. Coral reef ecosystems: how much greater is the whole than the sum of the parts? Coral Reefs 16 (Suppl.), S77–S91.

Hwang, D.-W., Lee, Y.-W., Kim, G., 2005. Large submarine groundwater discharge and benthic eutrophication in Bangdu Bay on volcanic Jeju Islan, Korea. Limnol. Oceanogr. 50, 1393–1403.

Kay, E.A., Lau, L.S., Stroup, E.D., Dollar, S.J., Fellows, D.P., Young, R.H.F., 1977. Hydrologic and ecologic inventories of the coastal waters of west Hawaii. Technical Report No. 105. Water Resources Center, University of Hawaii, Honolulu.

Kelly, R.P., Moran, S.B., 2002. Seasonal changes in groundwater input to a well-mixed estuary estimated using radium isotopes and implications for coastal nutrient budgets. Limnol. Oceanogr. 47, 1796–1807.

Kim, G., Burnett, W.C., Dulaionova, H., Swarzenski, P.W., Moore, W.S., 2001. Measurement of ^{224}Ra and ^{226}Ra activities in natural waters using a radon-in-air monitor. Environ. Sci. Technol. 35, 4680–4683.

Krest, J.M., Moore, W.S., Gardner, L.R., Morris, J.T., 2000. Marsh nutrient export supplied by groundwater discharge: evidence from radium measurements. Glob. Biogeochem. Cycles 14, 167–176.

Krest, J.M., Harvey, J.W., 2003. Using natural distributions of short-lived radium isotopes to quantify groundwater discharge and recharge. Limnol. Oceanogr. 48 (1), 290–298.

Lapointe, B.E., 1997. Nutrient thresholds for bottom-up control of macroalgal blooms on coral reefs in Jamaica and southeast Florida. Limnol. Oceanogr. 42 (5, pt. 2), 1119–1131.

Lapointe, B.E., O'Connell, J., 1989. Nutrient-enhanced growth of *Cladophora prolifera* in Harrington Sound, Bermuda: eutrophication of a confined, phosphorus-limited marine ecosystem. Estuarine, Coast. and Shelf Sci. 28 (4), 347–360.

Lau, L.S., Mink, J.F., 2006. Hydrology of the Hawaiian Islands. University of Hawai'i Press, Honolulu.

Li, L., Barry, D.A., Stagnitti, F., Parlange, J.-P., 1999. Submarine groundwater discharge and associated chemical input to a coastal sea. Water Resour. Res. 35, 3253–3259.

Moore, W.S., 1976. Sampling ^{228}Ra in the deep ocean. Deep-Sea Res. 23, 647–651.

Moore, W.S., 1996. Large groundwater inputs to coastal waters revealed by ^{226}Ra enrichment. Nature 380, 612–614.

Moore, W.S., 1999. The subterranean estuary: a reaction zone of ground water and sea water. Mar. Chem. 65, 111–125.

Moore, W.S., 2000a. Determining coastal mixing rates using radium isotopes. Cont. Shelf Res. 20, 1993–2007.

Moore, W.S., 2000b. Ages of continental shelf waters determined from ^{223}Ra and ^{224}Ra. J. Geophys. Res. 105, 22117–22122.

Moore, W.S., 2003. Sources and fluxes of submarine groundwater discharge delineated by radium isotopes. Biogeochemistry 66, 75–93.

Moore, W.S., Arnold, R., 1996. Measurement of ^{223}Ra and ^{224}Ra in coastal waters using a delayed coincidence counter. J. Geophys. Res. 101, 1321–1329.

Oki, D.S., Tribble, G.W., Souza, W.R., Bolke, E.L., 1999. Groundwater resources in Kaloko-Honokohau National Historical Park, island of Hawaii, and numerical simulation of the effect of groundwater withdrawals. U.S. Geological Survey Water-Resources Investigations Report 99–4070.

Paytan, A., Shellenbarger, G.G., Street, J.H., Gonneea, M.E., Davis, K., Young, M.B., Moore, W.S., 2006. Submarine groundwater discharge: an important source of new inorganic nitrogen to coral reef ecosystems. Limnol. Oceanogr. 51 (1), 343–348.

Precht, E., Huettel, M., 2003. Advective pore-water exchange driven by surface gravity waves and its ecological implications. Limnol. Oceanogr. 48 (4), 1674–1684.

Presto, M.K., Ogston, A.S., Storlazzi, C.D., Field, M.E., 2006. Temporal and spatial variability in the flow and dispersal of suspended-sediment on a fringing reef flat, Molokai, Hawaii. Estuarine, Coast. and Shelf Sci. 67, 67–81.

Prieto, C., Destouni, G., 2005. Quantifying hydrological and tidal influences on groundwater discharges into coastal waters. Water Resources Research 41, W12427.

Rama, Moore, W.S., 1996. Using the radium quartet for evaluating groundwater input and water exchange in salt marshes. Geochimica et Cosmochimica Acta 60 (23), 4645–4652.

Rama, Todd, J.F., Butts, J.L., Moore, W.S., 1987. A new method for the rapid measurement of ^{224}Ra in natural waters. Mar. Chem. 22, 43–54.

Robinson, C., Li, L., Barry, D.A., 2007. Effect of tidal forcing on a subterranean estuary. Adv. Water Res. 30, 851–865.

Shade, P.J., 1996. Water budget for the Lahaina District, island of Maui, Hawaii. U.S. Geological Survey Water-Resources Investigations Report 96-4238.

Shade, P.J., 1997. Water budget for the island of Molokai, Hawaii. U.S. Geological Survey Water-Resources Investigations Report 97-4155.

Shellenbarger, G.G., Monismith, S.G., Genin, A., Paytan, A., 2006. The importance of submarine groundwater discharge to the near shore nutrient supply in the Gulf of Aqaba (Israel). Limnol. Oceanogr. 51, 1876–1886.

Soicher, A.J., Peterson, F.L., 1997. Terrestrial nutrient and sediment fluxes to the coastal waters of west Maui, Hawai'i. Pac. Sci. 51 (3), 221–232.

Steven, A.D.L., Atkinson, M.J., 2003. Nutrient uptake by coral-reef microatolls. Coral Reefs 22 (2), 197–204.

Storlazzi, C.D., Jaffe, B.E., 2003. Coastal circulation and sediment dynamics along West Maui, Hawaii, Part I. U.S. Geological Survey Open-File Report 03-482. 28 p.

Storlazzi, C.D., Logan, J.B., McManus, M.A., McLaughlin, B.E., 2003. Coastal circulation and sediment dynamics along West Maui, Hawaii, Part II. U.S. Geological Survey Open-File Report 03-430. 50 p.

Storlazzi, C.D., McManus, M.A., Logan, J.B., McLaughlin, B.E., 2006. Cross-shore velocity shear, eddies and heterogeneity in water column properties over fringing coral reefs: West Maui, Hawaii. Cont. Shelf Res. 26, 401–421.

Umezawa, Y., Miyajima, T., Kayanne, H., Koike, I., 2002. Significance of groundwater nitrogen discharge into coral reefs at Ishigaki Island, southwest of Japan. Coral Reefs 21, 346–356.

Valiela, I., Costa, J., Foremand, K., Teal, J.M., Howes, B., Aubrey, D., 1990a. Transport of groundwater-borne nutrients from watersheds and their effects on coastal waters. Biogeochemistry 10, 177–197.

Valiela, I., Teals, J.M., Volkmann, S., Shafer, D., Carpenter, E.J., 1990b. Nutrient and particulate fluxes in a salt marsh ecosystem: tidal exchanges and inputs by precipitation and groundwater. Limnol. Oceanogr. 23 (4), 798–812.

Visher, F.N., Mink, J.F., 1964. Groundwater resources in southern Oahu. U.S. Geological Survey Water-Supply Paper 1778. 133 p.

Vitousek, P.M., Chadwick, O.A., Crews, T.E., Fownes, J.H., Hendricks, D.M., Herbert, D., 1997. Soil and ecosystem development across the Hawaiian Islands. GSA Today 7 (9), 1–7.